ICARUS: in-situ studies of the solar corona beyond Parker Solar Probe and Solar Orbiter

Vladimir Krasnoselskikh, Bruce T. Tsurutani, Thierry Dudok de Wit, Simon Walker, Michael Balikhin, Marianne Balat-Pichelin, Marco Velli, Stuart D. Bale, Milan Maksimovic, Oleksiy Agapitov, et al.

Experimental Astronomy (2022) 54:277–315
https://doi.org/10.1007/s10686-022-09878-1

ORIGINAL ARTICLE

ICARUS: in-situ studies of the solar corona beyond Parker Solar Probe and Solar Orbiter

Vladimir Krasnoselskikh · Bruce T. Tsurutani · Thierry Dudok de Wit · Simon Walker · Michael Balikhin · Marianne Balat-Pichelin et al. ***[full author details at the end of the article]***

Received: 13 August 2020 / Accepted: 25 October 2022 / Published online: 4 February 2023

Abstract

The primary scientific goal of ICARUS (Investigation of Coronal AcceleRation and heating of solar wind Up to the Sun), a mother-daughter satellite mission, proposed in response to the ESA "Voyage 2050" Call, will be to determine how the magnetic field and plasma dynamics in the outer solar atmosphere give rise to the corona, the solar wind, and the entire heliosphere. Reaching this goal will be a Rosetta Stone step, with results that are broadly applicable within the fields of space plasma physics and astrophysics. Within ESA's Cosmic Vision roadmap, these science goals address Theme 2: "How does the Solar System work?" by investigating basic processes occurring "From the Sun to the edge of the Solar System". ICARUS will not only advance our understanding of the plasma environment around our Sun, but also of the numerous magnetically active stars with hot plasma coronae. ICARUS I will perform the first direct *in situ* measurements of electromagnetic fields, particle acceleration, wave activity, energy distribution, and flows directly in the regions in which the solar wind emerges from the coronal plasma. ICARUS I will have a perihelion altitude of 1 solar radius and will cross the region where the major energy deposition occurs. The polar orbit of ICARUS I will enable crossing the regions where both the fast and slow winds are generated. It will probe the local characteristics of the plasma and provide unique information about the physical processes involved in the creation of the solar wind. ICARUS II will observe this region using remote-sensing instruments, providing simultaneous, contextual information about regions crossed by ICARUS I and the solar atmosphere below as observed by solar telescopes. It will thus provide bridges for understanding the magnetic links between the heliosphere and the solar atmosphere. Such information is crucial to our understanding of the plasma physics and electrodynamics of the solar atmosphere. ICARUS II will also play a very important relay role, enabling the radio-link with ICARUS I. It will receive, collect,

Grigory Vekstein is deceased.

✉ Simon Walker
simon.walker@sheffield.ac.uk

[1] LPC2E, CNRS/University of Orléans/CNES, Orléans, France

and store information transmitted from ICARUS I during its closest approach to the Sun. It will also perform preliminary data processing before transmitting it to Earth. Performing such unique *in situ* observations in the area where presumably hazardous solar energetic particles are energized, ICARUS will provide fundamental advances in our capabilities to monitor and forecast the space radiation environment. Therefore, the results from the ICARUS mission will be extremely crucial for future space explorations, especially for long-term crewed space missions.

Keywords Solar wind · Heliophysics · Solar atmosphere · Space mission

1 Introduction

The solar corona is crucial for understanding the process of the formation of the solar wind and consequently the Sun-Earth connections. It is still poorly explored, most of the studies by the Solar and Heliospheric Observatory (SOHO) and Ulysses were remote and distant, and just recently the measurements by Parker Solar Probe allowed to discover the complexity of the physical processes in the upper corona and in the region where the flow becomes sub-Alfvenic [1–3]. These studies clearly show that *in situ* measurements are necessary for further progress.

Hereafter, we propose a concept for a scientifically important space mission to explore the source of the solar wind from inside the solar corona at altitudes of between 2 and 60 R_S (solar radii).

Our primary science objective is to understand the processes that heat the solar corona and produce the solar wind and to determine the energy sources and paths for energy exchange between different components of plasma. ICARUS (Investigation of Coronal AcceleRation and heating of solar wind Up to the Sun), the concept of the mission we propose in response to ESA's "Voyage 2050" Call for science themes for future missions, will accomplish this objective with a combination of *in situ* particle and fields measurements onboard the ICARUS I satellite and a suite of remote sensing instruments onboard the ICARUS II satellite. The *in situ* instruments will measure all structures of various scales, including some of the smallest filamentary structures, transients, and waves in coronal holes and streamers along its trajectory. ICARUS I will enter the most important regions where the major energy dissipation occurs, to carry out *in situ* direct measurements in the area where the corona is heated and coronal plasma forms the solar wind for the first time. ICARUS I will cross most of the crucial regions in which both the slow and fast solar winds are formed. The remote sensing instruments onboard ICARUS II will detect both small-scale, transient magnetic structures and provide the global context and coronal conditions at the Sun and its environment during the crucial part of the closest approach of ICARUS I to the solar surface. To achieve these objectives we propose to carry out the following measurements:

1. *In situ* measurements
   - plasma distribution functions and ion composition;
   - plasma waves;

- electric and magnetic fields;
- neutron detector.

2. Remote sensing
   - magnetograph/Doppler (helioseismology) imaging of the Sun;
   - high spatial-resolution extreme ultraviolet / X-ray imaging of the Sun;
   - coronal imaging.

The mission and spacecraft designs are based on previously proposed concepts that were developed during earlier mission studies, namely Parker Solar Probe [4] and PHOIBOS [5]. This paper is an expanded version of the White Paper submitted in response to the ESA "Voyage 2050" Call.

1.1 Context

The primary scientific objective of the ICARUS mission will be to determine how magnetic field and plasma evolve in the solar atmosphere forming the corona, the solar wind, and the heliosphere. Achieving this goal will be a Rosetta-stone step for long standing fundamental astrophysical problems, that will shed light on not only the generation of the plasma environment of our own Sun, but also of the space plasma environment of numerous magnetically active stars, where hot tenuous magnetized plasmas are responsible for the energy transport and acceleration of particles over a wide range of scales. Moreover, by making the only direct, *in situ* measurements in the area where the processes of solar energetic particles energisation is initiated ICARUS will make unique and fundamental contributions to our ability to understand and predict the radiation environment in which future uncrewed and crewed space missions will operate

1.2 Why should we fly so close to the Sun's surface?

One of the last unexplored regions of the Solar System lies within 0.3 AU of the Sun. The goals of the Parker Solar Probe [4] (launched 2018) and Solar Orbiter [6] (launched 2020) missions are to study the solar wind inside and around this distance. Parker Solar Probe will approach as close as 9.8 R_S, and Solar Orbiter will approach to 0.3 AU but will move outside of the ecliptic plane to latitudes as large as 38°. Although Parker Solar Probe and Solar Orbiter will shed light on many questions concerning the solar wind heating and acceleration, the satellite trajectories, selected due to technical constraints, will fail to explore some critical regions in which important heating and acceleration processes take place. The most critical region is where the maximum energy dissipation occurs and the maximum of ion and electron temperature is supposed to be achieved. Both Parker Solar Probe and Solar Orbiter will miss this very vital space plasma region.

1.3 Analysis of the white light observations

White light brightness and polarization observations during solar eclipses have been employed to identify radial profiles of the solar corona electron density $n_e(r)$. The

gradient of $n_e(r)$ enables the determination of the density scale height H. Since H is proportional to the temperature, coronal temperatures have been determined at different heliographic latitudes and for different levels of solar activity. Several different methods have been used to determine the maximum temperature. They give comparable estimates of the maximum temperature about 1.1–1.5 MK. However there exist some differences in the heights at which this maximum will occur. Different methods of evaluation for the temperature profile provide quite strong arguments that the most significant fraction of the heating/acceleration of the solar wind occurs at altitudes of between 0.1 R_S and 2–4 R_S [7], i.e. sufficiently closer to the Sun than the closest distance to be achieved by the Parker Solar Probe and Solar Orbiter.

The physical processes that heat the solar wind are still poorly understood and are complex. One of the mysteries is related to the heating of the minor ions. Measurements of different UV spectral lines provide strong arguments that some of the ions, for instance O^{5+} may be heated up to temperatures one and a half orders of magnitude higher than the protons, that is, the ratio of temperatures may be larger than the mass ratio of ion components [8].

Another set of problems is related to the kinetic physics of the formation of particle distribution functions. It is well established that the electron distribution consists of several components, such as the core, strahl, halo, and super-halo. The effects of filtering [9], collisions, magnetic field divergence [10], wave activity, and intense macroscopic electric fields play important roles in the dynamics and formation of the different plasma components of the solar wind. However, current models are too simplistic to determine the relative role of these processes and their realistic characteristics, even for the case of the quasi-stationary solar wind.

Recent measurements by the Solar and Heliospheric Observatory (SOHO), Solar Dynamics Observatory (SDO), Hinode, and the Interface Region Imaging Spectrograph (IRIS) have shown evidence for the presence of a large number of dynamic features that make the formation of particle distributions even more complex. The solar corona is very dynamic and intermittent and the relative role of the different dynamic features, such as streamers or jets, in the formation of the slow and rapid winds is not completely clear. Moreover, the physical processes that form the solar wind take place in the chromosphere, a region that can currently only be studied by means of remote sensing. These processes are enormously important as one of the stages of the formation of the solar wind. Some quite important discoveries from the Hinode and IRIS satellites point to the importance of *in situ* studies of the characteristics of the plasma in the lower corona.

We do not have any direct experimental *in situ* measurements of processes in the regions where this formation takes place, and the current (SDO, Parker, Solar Orbiter) and planned future missions will not help us to solve all of these problems.

Until now these processes have only been studied by means of the remote sensing, and the regions where they occur are well inside 9 R_S. Thus it is rather improbable that Parker Solar Probe can study them *in situ*.

Other important regions are situated around the transition region from subsonic to supersonic flow. The flow in this region can be quite unstable and multiple instabilities capable of modifying the particle distribution functions may be present in these regions and may play quite an important role in the formation of particle

distributions. The studies of instabilities in the polar regions of the magnetosphere, in which the polar wind is formed, present quite strong arguments that the role of different types of plasma and magnetohydrodynamic (MHD) waves may be quite important. The study of wave particle interactions and wave activity *in situ* represent a very important problem in solar and solar wind physics.

1.4 Scientific objectives

At solar minimum the flow of solar wind may be separated into two distinct streams, known as the slow and fast solar wind, which exhibit typical velocities of about 400 km/s and 750 km/s respectively. Ulysses has shown that the high speed streams come from coronal holes and then, via superradial expansion, fill in the heliosphere. As the solar cycle develops, the latitudinal expansion of the streamer belt occurs. When solar maximum is reached, intermittent regions of fast and slow solar wind are uniformly distributed around the solar disc. This is illustrated by the 'dial plot' in Fig. 1 [11], which shows the latitudinal distribution of solar wind speed measurements during the first Ulysses orbit (corresponding to solar minimum) and its second orbit at solar maximum.

The fast solar wind originates from regions in which the coronal electron temperature is lower. This anti correlation of the solar wind velocity and the coronal electron temperature, where the freezing in of minor ion charge states occurs (Fig. 2), indicates that the basis of the original solar wind theory [12], i.e. that solar wind expansion is caused by the high coronal electron temperatures and electron heat conduction, may be presumably applicable only to the fast winds that originate from coronal holes.

The persistent positive correlation of *in situ* wind speed and proton temperature and very high temperatures of the coronal ions observed by SOHO indicate that other processes or forces, such as wave-particle interactions or the magnetic mirror force, may play a role in the expansion of the solar corona.

SOHO observations have added greatly to our knowledge of the slow solar wind. X-ray observations from Yohkoh show that the slow solar wind emanates from the magnetic activity belt and appears to continuously expand in a bursty, intermittent fashion from the top of helmet streamers. A third type of flow, arising from the eruption of larger coronal magnetic structures, i.e. coronal mass ejections (CMEs), creates shock waves whose leading edges create conditions for the acceleration of high-energy particles. Ulysses has shown that as the solar activity cycle progresses, the simple structure of regions of fast and slow solar wind gives way to a highly variable but typically slower solar wind at solar maximum.

The energy responsible for the heating of the corona and driving the solar wind is presumed to come from photospheric motions. The structure of the coronal plasma and photospheric magnetic fields is responsible for channeling, storage, and dissipation of this energy. Recent measurements from Hinode and IRIS led to the discovery of many dynamic jet-like features in the chromosphere, transition region, and low corona. For example, chromospheric anemone jets occur in active regions outside sunspots and possess typical dimensions of 2000–5000 km long and 150–300 kilometers wide [14] and exhibit an inverted Y-shape similar to that of the anemone

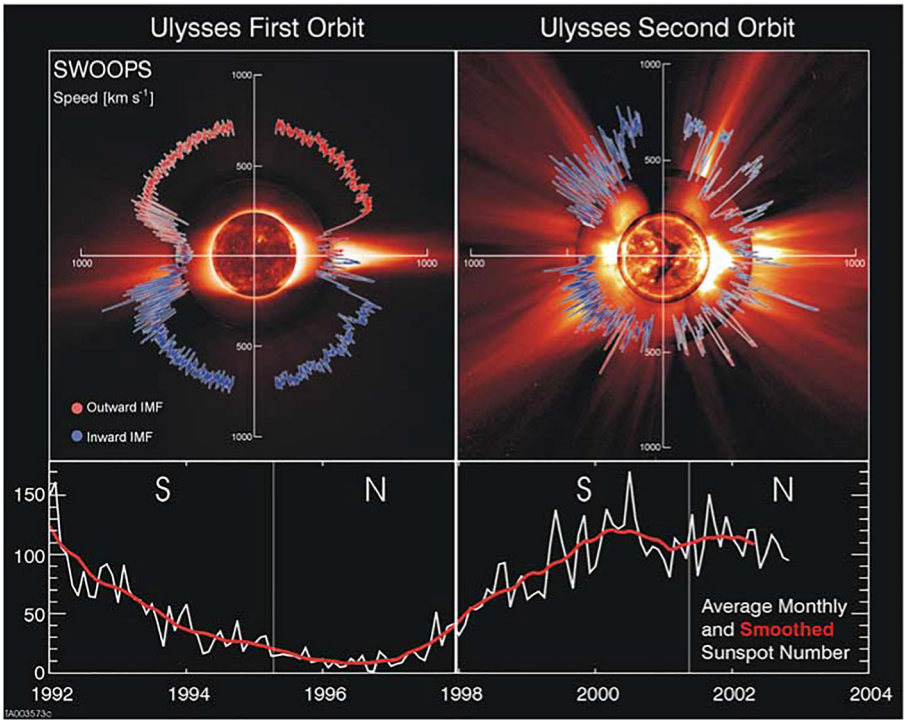

Fig. 1 Polar plots of solar wind speed as a function of latitude for Ulysses' first two orbits, superposed on solar images characteristic of solar min (8/17/96, left panel) and max (12/ 07/00, right panel), EIT, LASCO C2 images from SOHO, and Mauna Loa K-coronameter. These images show how the solar wind characteristics measured *in situ* depend strongly on the solar coronal magnetic field structure, fast wind emanating from coronal holes and slow wind appearing to originate from the magnetic activity belt. (Figure and caption from [11]). Copyright 2003 by the American Geophysical Union

jets observed in the corona that result from small-scale reconnection processes. Penumbral microjets, another class of fine-scale jet-like feature, typically have small widths (∼400 kilometers) and short duration of less than 1 minute. The identification of these events has proven to be quite difficult from existing observations. These microjets may probably result from magnetic reconnection processes within the complex magnetic configuration of sunspot penumbrae and may provide an important contribution to heating of the corona above a sunspot [15].

Fundamental plasma processes, such as waves, instabilities, magnetic reconnection, velocity filtration, and turbulent cascades, occur over a huge range of temporal and spatial scales and are presumed to be involved in the heating of the corona and acceleration of the solar wind. The lack of magnetic field measurements as well as detailed characteristics of the various plasma populations in the region inside 70 R_S hinders their validation or confutation at this time. Although Solar Orbiter will operate within 0.3 AU (60 R_S) and Parker Solar Probe as close as 9.8 R_S (in 2024), only ICARUS will be able to explore the critical regions within 10 R_S.

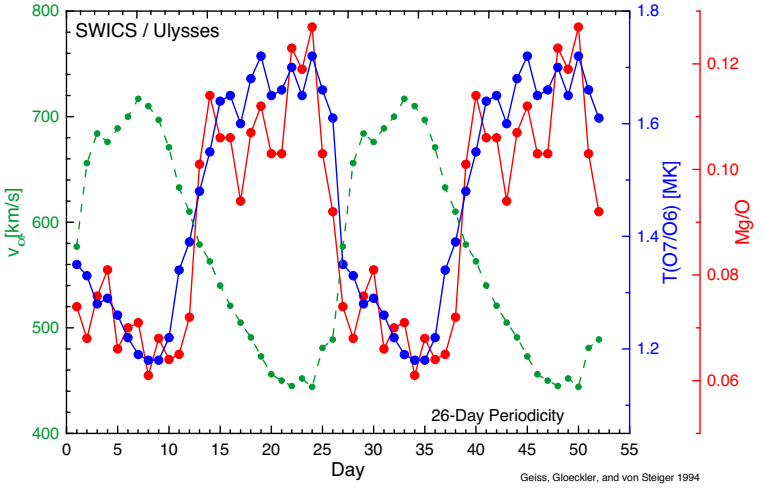

Fig. 2 Anti-correlation of solar wind speed (green dashed line) with the freezing in temperatures determined from O^7 to O^6 abundances (blue line), and magnesium to oxygen composition ratios (red line) as a function of time during a low-latitude high-speed low-speed wind crossing period in Ulysses' first orbit. (Figure and caption from [13])

Basic unanswered questions concern the storage, transport, exchange, and transformation to different forms before freeing up the mechanical energy necessary for coronal heating; the specific mechanism(s) for the conversion of energy between the magnetic field and thermal and nonthermal particle populations; the dynamics of photospheric and coronal magnetic fields in the source regions of the solar wind; and the sources of high-energy particles and the mechanisms by which they are accelerated.

These questions motivate three broadly distinct but interlinked top-level objectives for the ICARUS mission. An additional, exploratory objective would be to investigate the source, composition, and dynamics of dust in the inner Solar System. The role of dust, however, will not be addressed in what follows. Let us now discuss how the three main objectives translate into specific scientific questions and basic measurement requirements.

1.4.1 Objective 1: Explore the fundamental processes underlying coronal heating and solar wind acceleration

The mechanical energy associated with the convective motion in the photosphere is lost from the solar corona in the form of radiation, heat conduction, waves, and due to the change of the kinetic energy of the solar wind flow. The solar magnetic field plays a crucial role in the redirection, channeling, and storing this energy in the outer regions. However, the processes by which the energy is transferred, redistributed between different components of plasma, and dissipated to generate the hot corona, solar wind, and heliosphere over the development of solar cycles still is one of the fundamental unsolved problems in solar and heliospheric physics.

Remote-sensing observations of the solar corona and *in situ* measurements of the plasma distributions in the fast and slow flows of the solar wind have demonstrated that the thermalization is correlated with magnetic structure. The Doppler dimming technique (SOHO/UVCS) [16, 17] (Fig. 3) and interplanetary scintillation measurements [18] reveal that the high velocity solar wind is swiftly accelerated in the vicinity of the Sun, gaining velocities of around 600 km/s within the first 10 R_S. Studies of comet C/1996Y1 corroborate that the most likely solar wind velocity is around 720 km/s at 6.8 R_S [19].

It is presumed that the large, anisotropic effective temperature found in the solar corona leads to this fast acceleration. Moreover, some part of the heating has presumably already occurred in the upper chromosphere, which has been studied by SOHO/UVCS, IRIS, and Hinode. The perpendicular (to the magnetic field) temperatures are expected to be much higher. *In situ* measurements of the fast solar wind point to a possible remnant of this anisotropy, but less than that identified from coronal observations, but occurring at distances from 0.3 AU to 5 AU. The distributions of protons, alpha-particles, and minor ions in the fast solar wind also possess a non-thermal beam-like component whose velocity is similar to the local Alfvén velocity, and in the upper chromosphere may be even larger. All these features indicate a principle role played by Alfvén or ion-cyclotron waves in the processes of coronal thermalization to millions of degrees and solar wind acceleration in fast solar wind flows to hundreds of kilometers per second. One can mention the observations from the Hinode satellite that has provided quite important observations regarding the wave activity in the chromosphere. De Pontieu with co-authors [23] have pointed out that the observed wave activity of Alfvén waves is intense enough to provide the necessary energy source for the heating and acceleration of the solar wind. The high spatial and temporal resolution images produced by the Solar Optical Telescope (Hinode) have demonstrated that the chromosphere is filled with high amplitude Alfvén waves. Estimates of the energy carried by these waves and the comparison

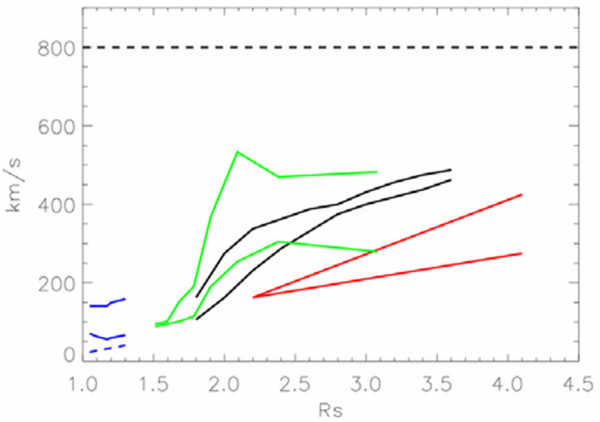

Fig. 3 Acceleration profiles of the fast solar wind after SOHO: H^0 (red) and O^{+5} (black) flow velocities from [17], O^{+VI} (green) flow velocities from [20]; Full-dashed blue lines: plume and interplume flow velocities from [21]. (Figure and caption from [22])

with advanced radiative simulations have demonstrated that these Alfvén wave possess sufficient energy to both accelerate the solar wind and feasibly to thermalize the quiet corona. *In situ* measurements close to the Sun, within the region in which the solar wind becomes super-alfvénic are necessary to remove any existing ambiguities in the mechanisms responsible for coronal heating and particle acceleration.

The occurrence of fluctuations of ∼50 km/s in the normally steady fast solar wind, together with the charge-state distributions, point to a low freezing-in temperature. The slow solar wind, on the other hand, is more variable and thus possesses a higher but variable freezing-in temperature. The fast and slow wind also differ in composition, with an over abundance of Fe and Mg with respect to O in the slow wind. The solar wind protons and ions of the high speed streams are typically hotter than those of the slow wind. The fast and slow solar wind streams also exhibit differences in the shape of the particle distribution functions at large distances from the Sun. The fast wind is characterized by slight proton anisotropic temperature distribution with $T_\perp > T_\parallel$. In addition, the main proton and alpha-particle populations are accompanied by beam populations with velocities comparable to the Alfvén speed. The fast and slow solar wind also differ in their turbulent characteristics. Fast streams contain strongly correlated transverse magnetic field and velocity fluctuations, typical of Alfvénic turbulence, and forming a well-developed spectrum of quasi-incompressible waves propagating away from the Sun. In contrast, the slow wind shows no preferred sense of propagation, while the larger magnetic field and density fluctuations that are present are more typical of standard and evolved MHD turbulent state [24].

The anti-correlation of electron temperature and solar wind velocity together with the heliospheric distribution of high speed flows at solar minimum (Fig. 2) indicate that coronal holes are the origin of the fast wind. Measurements from the CDS-SUMER experiment onboard SOHO have shown that the electron temperature is bounded by 10^6 K [25]. This corroborates measurements of the brightness temperature obtained from radio observations of the corona. This presents a discrepancy with the freezing in temperature for different ion charge states measured *in situ* by the SWOOPS experiment on Ulysses, the most direct interpretation of which requires an electron temperature maximum of about 1.5×10^6 K in coronal holes. The discrepancy may be resolved only by assuming strongly non-Maxwellian distribution functions for the electrons, or large differential flow speeds between ions of the same charge in the corona, which could have strong implications on the structure of the fast solar wind in the acceleration region. Such ideas have gained strong support through the observation of intense jets in the chromosphere and low corona by instruments onboard the IRIS and Hinode satellites.

In contrast to the proton distributions, the observed electron velocity distribution functions (eVDFs) display non-Maxwellian features regardless of the solar wind type (fast or slow). The eVDFs are composed of three different components: a thermal core surrounded by a supra-thermal halo that exist at all pitch angles, and a strahl component that is strongly aligned with the magnetic field and propagates in the anti-sunward direction [26]. The mechanisms responsible for energy dissipation and transport depend strongly on the mean free path of the coronal plasma particles and vary greatly with both radial distance above the base of the solar corona as well as the

spatial location within coronal structures such as coronal holes and helmet streamers. This dependence points to the fact that the heating of the upper corona results from the generation of non-thermal tails in the particle distribution functions. These high energy tails are produced between the chromosphere and the transition region, in which the solar plasma changes from being collisional to collisionless, probably resulting from magnetic reconnection processes and naturally culminating in higher temperatures and plasma outflows due to velocity filtration by the Sun's gravitational potential [27], and could probably explain the existence of the fast solar wind [28, 29]. Observations of differences in the fluctuations present in the fast and slow solar wind provide further evidence of the roles played by wave-particle interactions and turbulence in the process of coronal heating. Fast streams contain stronger fluctuations in transverse velocity and magnetic fields, and display a higher degree of correlation between the velocity and magnetic fluctuations (often described as a well-developed spectrum of quasi-incompressible Alfvén waves propagating away from the Sun). In the slow wind, this correlation occurs at a much lower level, while larger density and magnetic field magnitude fluctuations are present, indicating a more evolved MHD turbulent state there. This difference between the turbulent states of the fast and slow wind streams, coupled with the fact that slow wind distribution functions are much closer to equilibrium, suggests that the outward propagating wave flux contributes to the heating of the steady fast wind, while the slow wind is heated much more variably. However, it is currently unclear how the turbulent activity increases toward the Sun and whether it could provide sufficient power to heat the corona and accelerate the solar wind or how it changes with the occurrence of time-dependent events in the photosphere, chromosphere, transition region, and low corona (see e.g., [30]).

The mechanism responsible for coronal heating is a hotly debated topic, with proponents suggesting processes based on naturally arising motions in the photosphere or whether the dominant energy source resides in the currents stored via slower field line motions.

By combining IRIS observations with observations of the Swedish 1-m Solar Telescope (SST) De Pontieu and co-authors have demonstrated that in the solar chromosphere and transition region (TR) there is a prevalence of small-scale twist motions. It is supposed that most of the non-thermal energy that powers the solar atmosphere is transformed into heat in the chromosphere and transition region, although the detailed mechanism remains elusive. High-resolution (0.33-arcsec) observations with NASA's IRIS mission reveal that the chromosphere and TR are filled with twisting or torsional motions on spatial scales of the order of subarcsecond, within coronal holes, active and quiet regions. Coordinated studies with the SST enabled the quantification of these twisting motions and their relationship with fast thermalization to TR temperatures. Such studies of the interface region provide a new vision of the processes involved in the thermalization of the lower solar atmosphere. High levels of intense waves observed by IRIS may also presumably originate from reconnection events. The large gradients in the chromosphere and transition region imply that only Alfvén waves should exist. Slow waves would be expected to steepen and form shocks while fast waves undergo reflection. Transmitted waves propagate highly obliquely to the radial direction because of the large

Alfvén velocity, low frequencies, and strong structuring of the corona [31]. Therefore, the waves reaching the lower corona should be shear Alfvén waves, although discrete coronal structures e.g. plumes and loops may guide surface waves and propagate energy as global oscillations as well.

Numerical modelling demonstrates that in a strongly stratified atmosphere the nonlinear proceses that involve Alfvén waves originating from the photosphere possess the capabilities to form and maintain an incompressible turbulent cascade that exhibits the observed Alfvénicity. However, the effectiveness of the turbulence in channeling energy to dissipative scales is not resolved yet. The evolution of the spectral slope at different coronal heights (due to expansion and driving effects) impacts on the radial dependence of dissipation. The initial photospheric Alfvén wave spectrum cannot be identified unambiguously using *in situ* measurements in the far solar wind, since local processes contribute to its formation [32].

Only *in situ* measurements made within the corona will enable the Alfvénic spectrum to be constrained to advance our understanding of the contribution of turbulence to the processes of solar wind acceleration and the coronal theralization (Fig. 4).

By obtaining the first *in situ* data on plasma distribution functions, waves, electric and magnetic fields in the region from 1 R_S to 0.3 AU, and by relating them to the observed plasma and magnetic field structures, ICARUS will solve fundamental problems such as "What are the processes that energise the solar corona?, How the transfer of particle kinetic energy in the solar corona and wind occur?", and "What is the role of turbulence and wave-particle interactions in these processes?". Comprehensive measurements of plasma particle distribution functions and electromagnetic

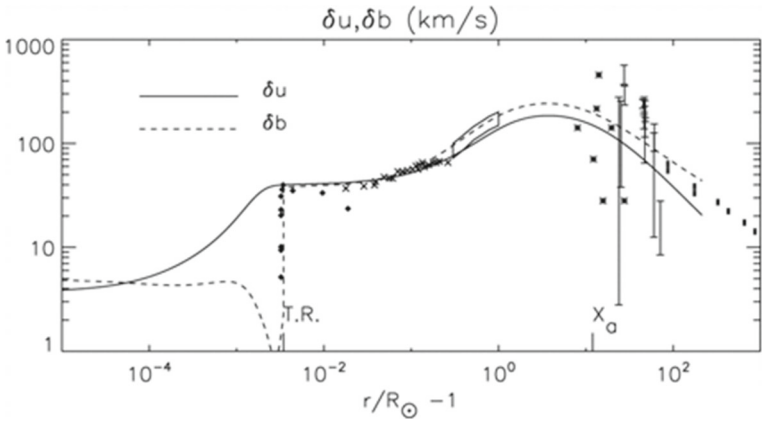

Fig. 4 The rms amplitudes δu (solid line) and δb (dashed line) in velocity units as functions of heliocentric distance for a photospheric Kolmogorov spectrum with $\delta u = 40$ km/s at the coronal base. The symbols indicate observational constraints imposed by measurements of nonthermal line-broadening velocities from SUMER of the disk (filled diamonds) [33] and solar limb (crosses) [34] , the box represents upper and lower limits from UVSC off-limb measurements [35], early measurements from [36], recent measurements of transverse velocity fluctuations using radio scintillation (bars) [37] and Elsässer energies from Helios and Ulysses (filled bars) [38]. ICARUS should reach inside the maximum fluctuation region, measuring spectra and correlations in the region of the data gap. (Figure from [39] and caption adapted from the same source) reproduced by permission of the AAS

fluctuations in the inner solar wind ($<20\ R_S$) will identify how the energy that powers the corona and wind is dissipated and what are the dominant dissipative structures, what are the spectra of electromagnetic variations.

Magnetic reconnection processes that occur on short scales play a significant role in ongoing theoretical models of dissipation in coronal plasma [40]. One of the important scientific investigations of ICARUS will be the studies of features of magnetic reconnection, such as bi-directional plasma jets, magnetic field, and velocity gradient correlations. *In situ* data gained by ICARUS in the corona and solar wind on the role played by turbulence, wave-particles interactions and nonlinear plasma dynamics will also have potential to make outstanding contributions to a wide range of fundamental astrophysical problems such as accretion discs, collisionless shocks occurring in the vicinity of supernova remnants, in galaxy-cluster formation, or associated with gamma-ray bursts.

Measurement Requirements:

- Macroscopic plasma characteristics:
  - 3 axes DC electric and magnetic fields;
  - Flow velocity, plasma density and temperature;
  - Particle distribution functions of protons, electrons and alpha particles;
  - Minor ions composition.
- Fluctuations:
  - Plasma wave measurements, spectra and snapshots of the waveforms of the magnetic and electric fields;
  - Plasma density fluctuations and determination of the gradients, when possible.

1.4.2 Objective 2: Determine magnetic field structure and dynamics in the source region of the fast and slow solar wind

The magnetic field lines determine the form of the flow tubes along which the conservation of mass and energy takes place. Therefore the evolution of the magnetic field from the photosphere up to a few solar radii controls the density distribution and velocity of the solar wind in solar wind models.

Data from the Ulysses mission has demonstrated that the radial component of the magnetic field in the fast wind does not exhibit a significant dependance on latitude. Therefore, latitudinal gradients in the average field occurring at the coronal base must be smoothed out by transverse expansion closer to the Sun. Flux tube expansion is a natural effect of the combined decrease in magnetic field and currents induced by the accelerating solar wind flow, and models suggest that it occurs out to radial distances $> 10 R_S$. Estimations deduced from Ulysses data indicate that the average polar magnetic field is about 6 G at solar minimum, however, magnitudes reaching up to 15 G in the photosphere cannot be excluded. Currently, there are no direct data of the polar magnetic field at altitudes below 1.5 AU [41]. By combining *in situ* measurements of the radial magnetic field along its trajectory with simultaneous remote

sensing of the polar photospheric magnetic field, ICARUS will provide a comprehensive view of solar wind expansion free from unknown parameters. ICARUS' data will enable the validation of existing models of coronal structure and identify the rigorous constraints for future models of the solar corona.

The magnetic network of the quiet Sun, as deduced from spectral lines formed at lower, transition region temperatures, is remarkably similar to the network in coronal holes, but its structure is significantly harder to resolve in lines formed at temperatures higher than 10^6 K. It seems to be quite probable that a similar coronal thermalisation process is operating for both coronal holes and quiet Sun. Therefore, it can be suggested that differences in their appearance are related to the magnetic field topology and possibly its time dependence. The higher densities, apparently hotter electron temperature, and different chemical composition of the quiet Sun would result from a difference of magnetic field configuration within the chromosphere and low corona compared to that which occurs in coronal holes. While signatures of coronal holes and equatorial helmet streamers are clearly observable in fast and slow wind streams and embedded plasma sheets, the effects of the corona of the quiet Sun are not as well known. Do closed magnetic field lines confine the plasma of the quiet Sun and therefore the entire fast solar wind originates from coronal holes? Another scenario would be that there is also mass loss from the quiet Sun. In this case what is its speed and how does its merging with the surrounding solar wind occur?

The magnetic field in active regions above sunspots confines the hot coronal plasma and is visible as intense X-ray loops that often possess cusp-like formations at their summit. At higher altitudes these evolve into streamers, which at solar minimum are elongated forming a belt around the magnetic equator of the Sun. Remote observations by SOHO/UVCS of the Extreme Ultraviolet (EUV) emission lines of minor ions, complemented by multi-fluid models, yield some pointers to the source regions of the slow solar wind in coronal streamers, but the magnetic field geometry and its role in plasma outflow are unclear.

The increase of solar activity within the solar cycle leads to an enhancement in the magnetic field structure complexity. Occurences of highly complex loop structures and streamers jutting out from the solar surface at all latitudes around the solar disc during periods associated with the maximum of solar activity are evident in observations. ICARUS will identify the regions in which the slow solar wind forms in relation to streamers and whether particular phenomena, such as embedded current-sheets, are related to its formation. Moreover, investigations of the sources of the solar wind during the maximum of solar activity will qualitatively identify any inputs to the solar wind from inside active regions. ICARUS will identify the geometry of the magnetic field within the active regions from which solar wind flow originates. ICARUS will pass over coronal holes, active regions and the quiet Sun at altitudes between 1 R_S and 20 R_S during various levels of solar activity. It will have the ability to trace the origin of the fast and slow wind and correlate the flow speed with the closed/open magnetic field topologies, as determined directly by photospheric field measurements as well as through indirect *in situ* measurements of any bidirectional streaming of electrons and energetic particles. The correlation of *in situ* coronal observations with surface features introduces the need for remote sensing of the solar disc, involving ecliptic viewing of the white light corona to allow the tracing of

field lines that cut the orbit of ICARUS I. These remote sensing observations will be provided by ICARUS II, which will provide simultaneous tomographic images from an all-sky coronagraph that can be used to identify coronal structures in the local spacecraft environment, together with a polar view of the photosphere and its embedded magnetic fields. These measurements will identify and locate the source region structures. It is essential that the ICARUS II payload includes instruments for coronograph-spectroscopic observations of both white light and UV. Recent measurements by the IRIS and Hinode satellites have shown quite unambiguously that coronal holes contain numerous kinds of different small-scale structures, confirming previous white light and UV coronagraph spectroscopic observations. Features such as bright striations, plumes, and microstructures can be traced from the solar surface to altitudes of 20 R_S. The relationship between plumes and the fast solar wind is poorly understood. Plumes, which appear above the X-ray bright points associated with coronal holes, are denser than the surrounding regions. An analysis of the UV lines observed in plumes indicates that they are narrower, which is evidence that the plasma in plumes is cooler than that in the regions separating them. It was shown that these latter features correspond to outflow regions [42]. Fine structures, such as micro-streams and pressure balanced structures are often observed in the fast wind and in coronal holes. These are radial velocity fluctuations with durations of about sixteen hours in the spacecraft frame and possess magnitudes of around 50 km/s. ICARUS I will fly through coronal holes at altitudes in the range from 1 R_S to 20 R_S from where it will cross coronal plumes or their remnants, estimating their filling factors, their overall contributions to the solar wind flow, and assess the expansion factors of the flow tubes that carry the solar wind flow. From these observations it should be possible to clarify how microstreams form and evolve and to determine their relationship to fine-scale coronal structures. To achieve this objective requires both *in situ* magnetic field, plasma velocity and full distribution function (density temperature and minor ion composition of solar wind) measurements to identify single flow tubes together with the use of tomographic reconstruction techniques from the all sky white-light coronagraph to provide information on the geometrical distribution and filling factor of the plumes.

Significant advances to our understanding of the origins of the slow solar wind streams around helmet streamers have been forthcoming from the LASCO and UVCS telescopes on SOHO. Sequences of difference images from LASCO collected around the sunspot minimum in 1996 appear to show quasi-continuous "puffs" of outflow material from the streamer belt [43]. Quantitative analysis of these moving features demonstrates that their origin is in the region above the cusp of helmet streamers and that they move radially outward with typical velocities of 150 km/s near 5 R_S which increases to 300 km/s at 25 R_S. The profile of the average velocity is consistent with the notion of an isothermal corona with a temperature T = 1.1 $\times$ 10^6 K (UVCS/SOHO measurements indicating temperatures of 1.6 $\times$ 10^6 K within the core of the streamer at solar max) with a critical point around 5 R_S. This ejection of plasma may be caused by the loss of confinement resulting from pressure-driven instabilities excited due to the accumulation of thermalized plasma or current-driven such as tearing and/or kink instabilities when the shear of the magnetic field in the streamer becomes large. The utilisation of a set of similar instruments onboard ICARUS II combined with the *in situ* measurements available from ICARUS I will provide unprecedented synergism

for the study of the dynamic characteristics of streamers and their role in coronal thermalization and formation of the solar wind. ICARUS I will traverse the streamer ejecta paths and discover whether the material ejected from the corona occurs either as a continuous flow or in puffs of disconnected plasmoids. In the case of the latter scenario, ICARUS will establish the plasmoid magnetic field configuration as well as the magnetic structure at the point of coronal disconnection. A comparison of radio data from Galileo and UVCS/SOHO images noticeably demonstrates a connection between the slow solar wind and the regions above the helmet streamer cusps that contain a current sheet (streamer stalks) [44]. However, it is unknown whether a single current sheet runs along the almost equatorial strip of maximum brightness in the white corona, i.e., along the streamer belt (as surmised by [45]), or whether there are multiple stalk/sheet structures that have a finite longitudinal extent. Nor is the structure of current sheets in streamer stalks known. Do they possess a simple structure, or are they composed of multiple sheets with a more complex magnetic field topology, as is suggested by UVCS/SOHO measurements [46] and the *in situ* observation of multiple current sheet crossings [47].

In situ measurements gathered far from the the Sun show that the solar wind is seen as a continuous flow of plasma. The quasi stationary nature of the solar wind may be associated with its features at the source. However, chromospheric and low corona observations (IRIS and Hinode) give strong argument in favour of the idea that it may result from a number of localised, impulsive phenomena that are distributed over smaller scales [48, 49]. Ample evidence exists for the "intermittent" or "pulsed" [49] nature of the fast solar wind: observations of microstreams and persistent beam-like phenomena in the high velocity solar wind; observations of interplanetary scintillations related to field-aligned density structures (with 10:1 radially-aligned axial ratio); evident field-aligned velocities in the range from ∼400 km/s to ∼1280 km/s [18, 50]; and remote sensing investigations of the corona, chromosphere and transition region displaying explosive, bursty events, multiple jets, and dubbed microflares, related to magnetic activity over very wide ranges of energy and time scales.

The fine scale phenomena detected in the high speed solar wind have been interpreted by [49, 51] as remnants of spicules, macrospicules, X-ray jets, and H-alpha surges. These authors suggested that the high speed solar wind originates from the superposition of transient jets caused by magnetic reconnection processes. If this hypothesis is correct, then the heating is time-dependent, leading to a time-dependent acceleration forming an ensemble of outgoing jets. It may be accompanied by the annihilation of oppositely directed magnetic flux bundles concentrated around magnetic network boundaries and is observed in the form of transient hard X-ray and gamma-ray bursts and neutron production in the 1-10 MeV range. ICARUS' scientific instrumentation possesses the capabilities to survey these phenomena. There are also plenty of arguments in favour of an intermittent origin of the slow solar wind. Many models have been developed for the loss of plasma blobs by helmet streamers positioned above active regions. At solar maximum the non-stationary variability of the wind is determined by CME's and fine-scale structures originating from active regions. In such conditions the flow becomes spatially structured. More generally one can say that CME-like events at all scales play an important role in the formation of the intermittent solar wind. In order to fully comprehend the processes occurring in

the solar wind source region, the *in situ* data gained in close proximity to the Sun are required to provide information about the structure of the solar wind, the distributions of plasma components (both ions and electrons) and the varying abundances of various elements in the solar wind.

The proposed scientific instrumentation of ICARUS I is capable of measuring electron/ion distributions and bulk velocities of minor ion constituents in the coronal hole. During perihelion passages, ICARUS will gain *in situ* data on the disparities of the composition in regions of closed and open magnetic field.

In performing continuous measurements of the characteristics of the plasma flow while approaching the Sun to closer than 10 R_S ICARUS I will be able to characterize the intermittent properties of the fast and slow solar wind and their evolution with the distance. Direct *in situ* measurements from the Parker Solar Probe has shown that the time variability of the flow may significantly increase closer to the Sun, even during quiet Sun time periods [1, 2]. During active times it may become much more important. Techniques for the determination of the connectivity of *in situ* measurements with lower corona and the photosphere will enable the identification of the relationship between physical processes occurring in the lower layers of the corona, and those observed in the transition region, photosphere and at larger distances. This would allow the establishment of the origin and sources for the variability of the wind observed *in situ* locally at lower levels of the corona and photosphere, in particular by bursty events or micro-CME's, or by interchange reconnection [52]. It was also shown using data from the Parker Solar Probe that such events may be analyzed in more detail by incorporating images made by an all sky camera onboard the satellite together with images obtained by other satellites at Earth orbit. An important step forward that was made by analyzing the sources and origin of the solar wind using Parker Solar Probe data was the excellent ability to reconstruct the connectivity between *in situ* measurements and the lower corona making use of potential field source surface modelling [53]. It was also demonstrated that the directivity of the electron fluxes provides important information regarding the open/closed structure of the magnetic field lines. Note that for fast particles, aberration is due to (delta b/B) (maximum estimated in the range 0.2 – 0.3). In coronal holes, filamentary structures such as coronal plumes are observed up to $30R_S$, the range of speeds at perihelion implies speeds across plumes in the range 100 – 200 km/sec. With an expected size less than $10^3 - 10^5$ km at $8R_S$, the crossing time of an individual plume should last between 5 seconds to 1 hour. During that time one must ensure continuous measurements of the plasma characteristics, particle density, and velocity measurements. Radio measurements at the plasma frequency are also essential to give a separate and independent measure of density, speed and temperature of the core of the electron distribution function.

Measurement Requirements:

- Full distribution functions of electrons and ions measurements, including measurements of strahl;
- Measurements of energetic ions composition;
- *In situ* magnetic and electric fields in inner heliospheric regions at high cadence in inner heliospheric regions (below 20 R_S);

- Continuous, lower cadence measurements below 0.3 AU;
- High energy tails of proton and helium distribution functions at high cadence;
- Time-dependent neutron and gamma-ray energy spectra;
- Photospheric magnetic field at high latitude and line of sight velocity fields;
- All sky coronograph measurements of coronal structure above 10-20 R_S onboard ICARUS II;
- Spectroscopic measurements with EUV spectrograph onboard ICARUS II.

1.4.3 Objective 3: What mechanisms accelerate and transport energetic charged particles?

Solar Energetic Particle events (SEPs) may be separated into two distinct categories: Gradual and Impulsive. Particle acceleration by collisionless shocks associated with CMEs leads to gradual SEP events. These events possess abundances and charge states similar to those of the corona. Impulsive events are generally weaker and are related to acceleration during magnetic reconnection events. They can be associated with impulsive X-ray flares and exhibit enrichments in ^{3}He and heavy ions (e.g., Fe) with charge states corresponding to energies in the range from ∼5 to 10 MK. Both reconnection and CME shock driven acceleration processes are known to occur in stronger SEP events. Studies of the SEP events that occurred during the 23rd Solar Cycle reveal that features of both gradual and impulsive SEP are frequently observed (e.g., [54–56]). Moreover, measurements at 1 AU point to a continuous outflow of particles from the Sun with intermediate energies extending from suprathermal to >10 MeV/nucleon, in addition to SEP events. The processes that are responsible for the acceleration of these particles are not known yet.

On the basis of data gained at 1 AU it is very problematic to separate the diverse processes of acceleration that occur close to the Sun. The propagation of the interplanetary plasma from the Sun to 1 AU alters the temporal structure of events, curtails their intensities, and results in the blending of particles accelerated by different mechanisms. However, since its orbit will take it to altitudes as low as 1 R_S, ICARUS will sample energetic particles close to their local acceleration site within the solar corona and inner heliosphere before they lose their temporal characteristics due to propagation effects. Recent results from WIND, SOHO, and ACE indicate that the high corona ($2R_S < r < 20R_S$) is an important site for the acceleration of both ions and electrons. ICARUS I will carry out *in situ* measurements within this region that may be used to address key questions related to the acceleration and transport of SEP.

The use of simultaneous observations at 0.3 AU and 1 AU will enable the observations by ICARUS I to be traced back to the original flare site and hence allow the characteristics of the flare site, such as the magnetic field configuration, to be elucidated. Additionally, ICARUS I will observe near-relativistic electrons with speeds $V > 0.1$ c within a few seconds of their generation by their progenitor event. Observation of these high energy electrons is important as the acceleration sites responsible may be observed remotely by their associated microwave or hard X-ray emissions. In the case of ion acceleration, ICARUS I will be able to observe gamma rays and neutrons produced by solar flares and hence enable the investigation of particle acceleration on the closed field lines within the solar atmosphere.

Observations show that the rate at which SEP events occur is greatly diminished during solar minimum. Despite this, there is strong evidence to indicate that particle acceleration occurs continuously at the Sun and inner heliosphere. All ion species (e.g. H^+, He^+, and He^{++}) observed in the solar wind possess suprathermal tails extending up to several times that of the solar wind speed ($\sim$10 keV/nucleon). Such tails in the distributions are present continuously, even during periods when solar activity and interplanetary shocks are absent. These tails are more conspicuous in observations from the ecliptic than from polar observations (e.g., [57]). Suprathermal tails are also observed in distributions of interstellar pickup ions such as He^+, suggesting that they are accelerated within the inner heliosphere (e.g., [58]). Solar observations by RHESSI show the continual acceleration of ^{3}He, even during less active periods, suggesting that acceleration occurs more or less continuously in microflares [59]. The occurrence of random, small scale component reconnection, a characteristic of microflares, may be indicative of the occurrence of scale-invariant dissipative processes that not only heat the coronal plasma but also give rise to a stochastic electric field component that plays a part in the acceleration of particles. Observations of neutrons, gamma, and hard X-rays made by ICARUS I will shed light on the occurrence of continuous and sporadic processes of particle acceleration. The low energy neutron observations by ICARUS I are of special interest since these particles do not propagate to 1 AU and so may only be observed in the vicinity of the Sun (the intensities of $\sim$1 MeV(10 MeV) at 5 R_S are $\sim 1.5 \times 10^{10}$ (3.7×10^6) times greater than at 1 AU). Neutron measurements from a vantage point close to the Sun may provide evidence for the existence of small nanoflares, events that have also been put forward as an important process for coronal heating.

To enable the reliable forecast of large SEP events, it is essential to understand the process in which particles are accelerated by CMEs and why some events are more efficient than others. Several suggestions have been made such as (1) the presence or absence of a pre-existing population of suprathermal ions, left over either from a previous gradual event (e.g., [60]) or from small impulsive flares [61]; (2) the presence or absence of successive, interacting CMEs [62]; (3) pre-conditioning and production of seed-particles by a previous CME [60]; (4) improved injection efficiency and acceleration rate at quasi-perpendicular (as opposed to quasi-parallel) shocks [56]; (5) variable contributions from flare and shock-accelerated particles [55], including acceleration of associated flare particles by the shock [63, 64]; and (6) production of SEPs in polar plumes, where shock formation may be easier [65].

Analysis of respective time sequences has shown that gradual SEP events are initially accelerated at altitudes between $\sim 3\ R_S$ and $12\ R_S$ [66] suggesting that SEPs originate above $\sim 3\ R_S$. The reason behind this is that the Alfvén velocity peaks at $\sim 3\ R_S$, implying that for typical CME speeds, shocks may be easily formed and sustained beyond this radius (e.g., [67]). MHD simulations of coronal shock driven SEP events (e.g., [68, 69]) need to either make assumptions or model the solar wind and Alfvén speeds, density profiles, magnetic field, density of seed particles, and turbulence levels that control the particle diffusion coefficient in which gradual SEP events originate. It is currently not known why, for a given CME speed, the peak intensity of $>$ 10 MeV protons can vary by a factor of $\sim 10^4$ [60]. ICARUS I will measure the solar wind and magnetic field close to the Sun, the density and energy spectrum of

suprathermal seed particles, and the spectrum of magnetic turbulence directly. It will enable us to ascertain the presence of shocks and discontinuities and determine their role in particle acceleration.

The probability that ICARUS will encounter particle intensity levels characteristic of large SEP events at 1 AU (e.g., >100 particles $cm^{-2}sr^{-1}s^{-1}$ with E >10 MeV) is about 80% during solar maximum conditions [70]. It is much less likely, however, (∼10-20% probability) that the ICARUS I flyby will take place while a CME-driven shock is accelerating >10 MeV particles inside 100 R_S. Nonetheless, ICARUS measurements of the ambient conditions that exist prior to such events will be of enormous value to our efforts to understand SEP acceleration and transport.

Ulysses has demonstrated that SEPs can be observed at high latitudes [71]. Currently, three explanations for these observations have been proposed: (1) the CMEs responsible for accelerating these particles extend to high latitudes, crossing interplanetary magnetic field lines connected to Ulysses; (2) significant particle cross-field diffusion occurs and (3) magnetic field lines connecting low latitude active regions to high latitudes exist within the solar corona, enabling particles close to the Sun to reach high latitudes. Comparison of the onset times at Ulysses with those in the ecliptic for events with the same solar origin [72] concluded that events observed at high-latitude are not consistent with processes involving direct scatter-free propagation along a magnetic field line. The large path lengths and late release times indicate that propagation to high latitudes requires scattering. By employing a polar trajectory ICARUS will encounter energetic particles at all latitudes. This will enable the determination of the scattering properties of particles from the corona into the solar wind and their dependence on magnetic field and turbulence intensities. These measurements will also identify large-scale deviations from the Parker spiral configuration (Objective 2) and determine their role in energetic particle scattering.

Both impulsive and gradual SEP events give rise to energetic electrons. Since the electrons possess near-relativistic velocities, the onset times of electron events at 1 AU can be used to determine SEP release times in the vicinity of the Sun which may then be compared with their associated electromagnetic signatures. It is found that, surprisingly, these release times are nearly always delayed by ∼10 minutes with respect to their associated electromagnetic (soft X-ray and optical emissions from flares and associated radio emissions) signatures (e.g., [73, 74]). This has initiated considerable debate concerning its cause. Proposed mechanisms include (1) storage and subsequent release of the electrons, (2) the longitudinal propagation of the acceleration region from flare site to injection site, (3) radial transport of the acceleration region due to e.g. a CME-driven shock [74]. By passing close to the Sun ICARUS will find itself in a region in which propagation delays will be minimized, and energetic electron measurements combined with interplanetary magnetic field observations will reveal where and how particles are released from the Sun and/or accelerated in inter-planetary space.

Measurement Requirements:

- High-energy ions and electrons;
- *In situ* vector magnetic field;
- Remote sensing of active regions, flares, solar radio bursts, and CMEs;

- Basic plasma parameters (proton, alpha particles) and electron thermal and suprathermal distribution function;
- Composition minor ion distribution function extending to high-energy tails;
- Composition and spectra of energies through ∼100 MeV/nuc, including ^{3}He;
- Plasma waves measurements and electron density, temperature, and velocity;
- Magnetic and electric fields and plasma density fluctuations;
- Analysis of correlations with underlying magnetic structure obtained from imaging.

2 Mission profile

The primary scientific objectives of the ICARUS mission require direct *in situ* measurements of plasma parameters, particle flows, electromagnetic fields, wave activity, and energy flows in the regions where the solar wind is generated. These measurements should be performed where both fast and slow wind are created. In order to satisfy these conditions ICARUS I will fly as close as technically possible to the solar surface.

The single most important defining parameter of the mission is the distance to the Sun at perihelion. The scientific output versus closest distance to the Sun can be summarized in Table 1, in which we consider mission profiles for different distances from the Sun.

Since there is a clear optimum between 1 and 2 R_S, we propose the perihelion to be at 1 R_S from the solar surface (i.e. 2 R_S from the centre of the Sun). Another requirement, penetrating and crossing regions of the fast and slow wind generation, imposes that the trajectory of ICARUS I should be in the plane perpendicular to the ecliptic and it will orbit the Sun either from the North pole to the South, or vice versa. The closest distance may be slightly relaxed if the conditions for measurements due to the degassing of the thermal shield will make scientific measurements too polluted. The results of the direct *in situ* measurements will be immediately directly

Table 1 Relevance of the mission for the various key questions versus closest distance to the Sun

Distance from the Sun	$< 1R_S$	$1-2R_S$	$2-4R_S$	$4-10R_S$
How is the solar wind accelerated?	relevant	very relevant	very relevant	relevant
How is the solar wind heated?	relevant	very relevant	very relevant	incremental
What are *in situ* properties of the solar atmosphere?	very relevant	very relevant	relevant	incremental
Feasibility	not possible	$> 1.5R_S$ possible	possible	possible
Mission objective	too challenging	target objective	backup objective	not innovative enough

transmitted to ICARUS II by the X-band antenna. These measurements should be completed by remote sensing, namely, by white light all-sky optical measurements, by magnetic field measurements to connect local fields around the ICARUS I trajectory with magnetic configuration in the photosphere and chromosphere, and by EUV/UV measurements providing information about surrounding flows. These tasks will be accomplished by the second satellite of the mission, ICARUS II. It will also ensure a very important role of the relay. Close approach to the Sun will result in strong scattering of the emitted radio signal. To obtain good enough signal to noise ratio the receiver should be placed not too far from ICARUS I. A desirable trajectory for ICARUS II may be in the equatorial plane with perihelion about 0.3 AU. During the critical phase of ICARUS I's approach to the Sun ICARUS II should be not far from the line perpendicular to the plane of the trajectory of ICARUS I to observe it all the time and to have good conditions for remote sensing measurements. The precise positioning of ICARUS II may be specified after additional analysis of the quality of the transmission-reception of the information by ICARUS I during the critical phase of its closest approach to the Sun. The schematic figure of the satellite trajectories is presented on the Fig. 5.

2.1 ICARUS I

ICARUS I comes close to the Sun with a perihelion altitude of 1 R_S. In order to achieve the scientific objectives of the mission it will perform direct *in situ* measurements of all major parameters of plasma, electromagnetic fields, flows, wave activity, X-ray, and slow neutrons along its trajectory. It should be in the plane perpendicular to the ecliptic passing from the South to North pole (or vice versa). The critical phase of its mission will be during its closest approach to the Sun from about 30 R_S from one pole to ~30 R_S from the other. Solar wind generation, both in the equatorial region and coronal holes, must be studied. These two areas are supposed

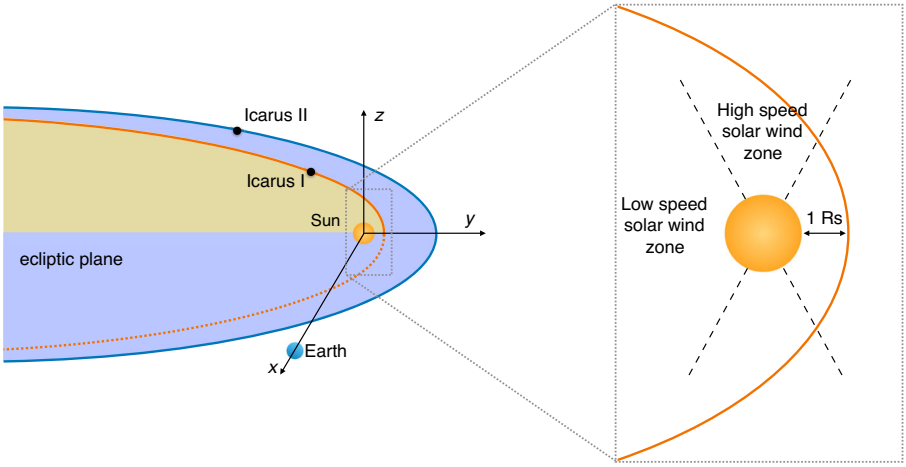

Fig. 5 Schematic representation of the trajectories of the ICARUS I and ICARUS II satellites during the crucial phase of the ICARUS I satellite trajectory

to be the sources of the slow and fast solar wind. Probing both types of the winds the satellite will also investigate the properties of boundary regions between the two and will study their characteristics. Its unprecedentedly close approach to the Sun will also create a unique opportunity to carry on measurements of neutrons in the close vicinity of the Sun that decay very rapidly and may not be detected by any other satellite. They are very important in the determination of small-scale physical processes producing high energy particles such as micro- and nano-flares. ICARUS I will be completely focused on *in situ* measurements and from 20–30 solar radii until returning to the similar distances around another pole of the Sun it will perform rapid measurements of plasma distribution functions, from thermal to non thermal and energetic tails, energetic minor ions fluxes and composition, electric and magnetic fields, neutron and X-ray fluxes. It will register the data of measurements into the common Data Processing Unit (DPU) that will encode and transmit to the ICARUS II immediately. The satellite will be protected by the cone type heat shielding (opening angle 15°). The extremely high satellite speeds (about 450 km/s; Fig. 6) in the vicinity of perihelion almost perpendicularly to the radial direction to the Sun is significantly higher than the theoretically expected solar wind speeds. Thus the plasma and low energy energetic particles will enter the spacecraft umbra from the side of the spacecraft that is facing forward.

This mission concept will allow the use of standardized, miniaturized instrumentation which in turn allows low weight and power. The particle fluxes are quite large, which will result in quite good statistics for particle measurements. On the other hand, such parameters as Debye length evaluated from existing models [75] and presented on Figs. 7 and 8 for equatorial and coronal holes regions are rather similar to those in the ionosphere, from tens of centimeters to several meters that signifies that the characteristic length of electric field antennas and booms for magnetic field and particle sensors may be quite similar to those used already in other space missions. Table 2 lists the baseline scientific payload for ICARUS I.

According to a preliminary study of Y. Langevin (Private communication, 2016), the one and only way to achieve such a close solar distance is the initial scheme

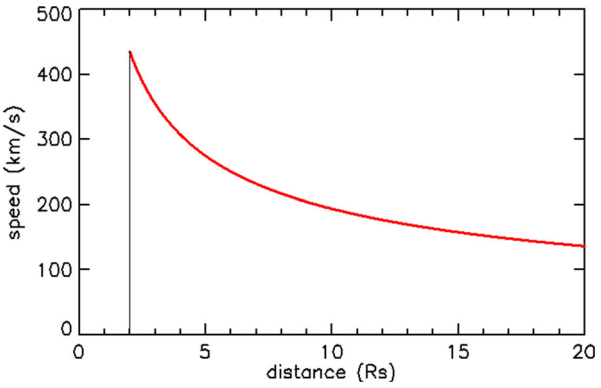

Fig. 6 Schematic velocity dependence upon distance to the Sun around perihelion of the ICARUS I trajectory

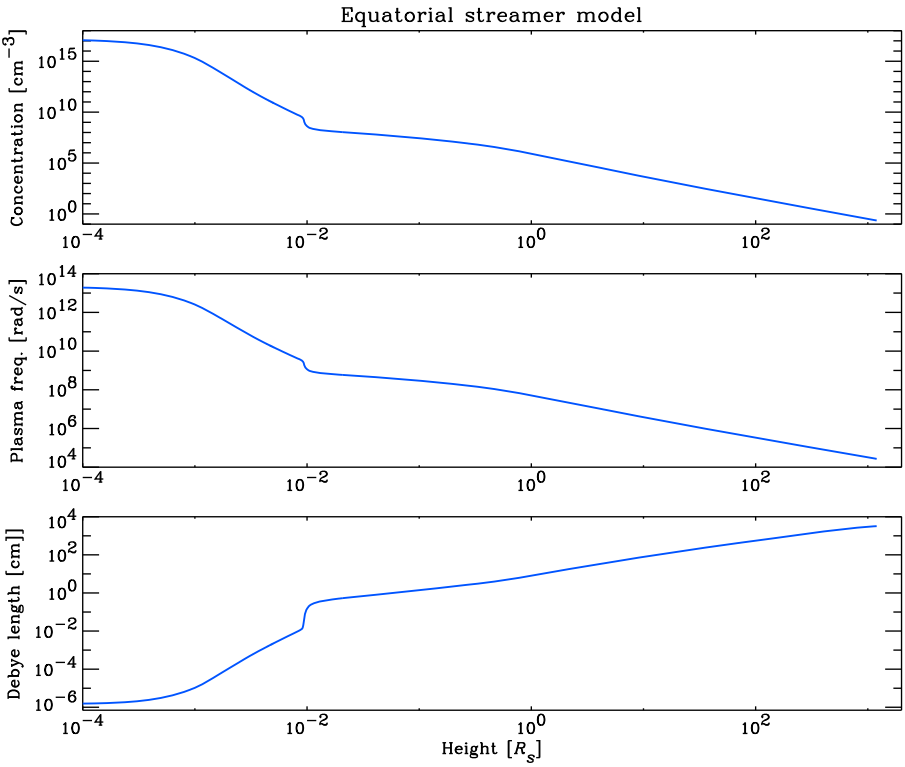

Fig. 7 Plasma density, plasma frequency, and Debye length as a function of the distance from the solar surface obtained in simulations for equatorial regions. These plots are based on [75]

for NASA's Parker Solar Probe mission, i.e., reaching Jupiter with a velocity of $\sim$12 km/s and using a gravity assist at a distance of $\sim$700, 000 km (still acceptable even if there is some radiation dose incurred) to turn it opposite to Jupiter's orbital velocity. Solar electric propulsion or solar sail cannot work, as such low thrust schemes require a very extended spiral (combined or not with Venus gravity assists) and the solar sail (or solar panels) would be burned out much before reaching the target distance, which corresponds to a hefty solar energy flux of 16 MW/m^2.

The simplest way to achieve this is to use a NASA Atlas-Centaur launcher. The 504 version was needed for launching either New Horizons or Parker Solar Probe with a departure velocity of 14 km/s. There is a direct window to Jupiter every 1.1 years which requires a launch velocity of $\sim$10.2 km/s for reaching Jupiter at $\sim$12 km/s. The total duration to the close solar pass is of the order of 3.5 years. One can decrease the number of boosters as the launch velocity for ICARUS is smaller than for Parker Solar Probe. If the probe survives the first pass then one could have a second pass after 4 years.

There exist solutions with European launchers as well, but the mission timelines are longer.

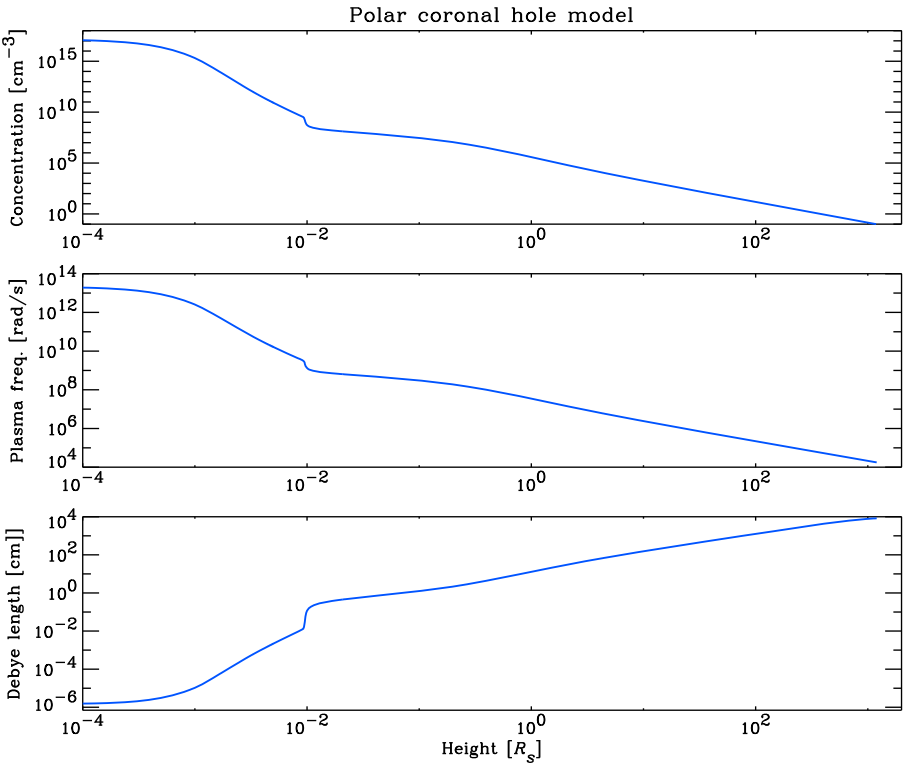

Fig. 8 Same as Fig. 7, for coronal holes. Based on [75]

2.2 ICARUS II

ICARUS II will approach the Sun to the distance of approximately 60 solar radii from its surface. It should accomplish two major important tasks complementary to those of ICARUS I. During the critical phase of the ICARUS I trajectory close to perihelion ICARUS II will perform remote sensing measurements focused on the regions where ICARUS I moves. Its measurements of parameters such as density, temperature, magnetic field etc. around regions along the trajectory of ICARUS I are crucial for understanding physical processes of the generation of solar wind. ICARUS II measurements will complete *in situ* local measurements. The important parameters necessary for interpretation of *in situ* local measurements are magnetic field configuration and spectroscopic measurements of EUV emissions.

Remote observations of the magnetic field are needed to reveal the surface field configuration of the surface magnetic fields related to various coronal and solar wind phenomena. Observations of the magnetic field at the borders between coronal holes and streamers will shed light on the contributions of open and closed magnetic field configurations in the generation of the slow solar wind. Therefore, to achieve its scientific goals, the remote observations of the magnetic field are needed.

Table 2 Baseline instrument and resource requirements for the ICARUS I satellite

Instrument	Mass (kg)	Power (W)	Peak Data Rate (kbps)
Fast Ion Analyzer (FIA)	2.5	3.7	10
Fast Electron Analyzer (FEA)	5	7.2	20
Ion Composition Analyzer (ICA)	6	6	10
Magnetometer (MAG)	1.5	2.5	1.1
Radio and Plasma Wave Instrument (RPWI)	7	10	4
Energetic Particle Instrument, Low Energy (EPI-Lo)	1.5	2.3	5
Energetic Particle Instrument, High Energy (EPI-Hi)	2.5	1.7	3
Neutron/Gamma-Ray Spectrometer	2.5	3.0	0.5
Common DPU/Low Voltage Power Supply	10	14	N/A

To assess the parameters (temperature, density, flow velocities, occurrences of waves and turbulence) related to various solar wind structures measurements of the UV/EUV spectra are needed. Spectroscopic measurements of coronal outflow bulk speeds at the borders between coronal holes and streamers will assist to study the contributions of open and closed magnetic field configurations in the thermalisation of the slow solar wind. In addition, EUV spectra would also yield significant details regarding solar wind structures. Spectra of the waves and turbulence in coronal structures can be identified using measurements of the velocity distributions of ions and electrons. Doppler shifts and abundances of ions can be determined in order to assess the fast and slow solar wind source regions.

ICARUS II will measure also energetic particles and their composition. This will allow their transport in the inner heliosphere to be traced.

The second important task consists of receiving, collecting, and storing the data that ICARUS I will transmit in the regime of direct transmission immediately after

Table 3 Baseline instrument and resource requirements for the ICARUS II satellite

Instrument	Mass (kg)	Power (W)	Peak Data Rate (kbps)
Magnetometer (MAG)	1.5	2.5	1.1
Energetic Particle Instrument, Low Energy (EPI-Lo)	1.5	2.3	5
Energetic Particle Instrument, High Energy (EPI-Hi)	2.5	1.7	3
Coronal Dust Detector	1.5	3.8	0.1
Hemispheric Imager (HI)	1.5	4.0	70
Polar Source Region Imager (PSRI)	3.5	4.0	70
Common DPU/Low Voltage Power Supply	10	14	N/A
Extreme Ultra-violet spectrometer (EUVS)	TBD	TBD	TBD
Magnetograph (MG)	TBD	TBD	TBD
Coronagraph (CG)	TBD	TBD	TBD

registering *in situ* measurements. The data transmission from the regions close to the Sun may undergo an extremely high level of scattering, thus the relay through the receiver that will allow good quality of data transmission will be quite important for the success of the mission. These data then will be re-transmitted to the Earth. This role of relay implies that ICARUS II should be placed along the line almost perpendicular to the plane of the ICARUS I trajectory (see Fig. 5). It should have onboard high quality and as large as possible memory to store the data. To obtain maximum outcome from remote sensing the sampling rate of magnetograph and spectroscopic measurements should be quite high. This issue should be addressed during preliminary study of the project feasibility. It is also necessary to have an onboard high quality X-band receiver. ICARUS II can have an onboard additional optional instrument for the studies of dust in the heliosphere. A baseline scientific payload for ICARUS II is listed in Table 3.

The trajectory of ICARUS II may be in the ecliptic plane and it can be determined using the studies of trajectories for the Solar Orbiter mission.

2.3 Baseline payload

We present hereafter a short description of the payload proposed for the PHOIBOS Mission [5] that may be used as a baseline for the ICARUS I payload.

2.3.1 Fast plasma instrumentation

There are several basic requirements for the measurement of the coronal thermal plasma. The ion instrumentation should be able to distinguish alpha particles from protons under all conditions. The field of view (FOV) coverage for the distribution functions should be as complete as possible. The basic moments of the distributions, density, velocity, and temperature should be obtained fast enough and accurately enough to enable the possibility to analyze Alfvénic and MHD turbulence.

The ICARUS I Fast Plasma Instrumentation will consist of a single Fast Ion Analyzer (FIA) and a pair of Fast Electron Analyzers (FEAs). These instruments are similar to those operating onboard the Solar Orbiter project of ESA [76].

FIA is similar to the ion composition analyzer that is integrated into the Solar Wind Analyzer (SWA) accommodated onboard the Solar Orbiter spacecraft [76].

The FIA and one of the FEAs may be mounted, together with the Ion Composition Analyzer (ICA), on a movable arm on the ram side of the spacecraft; the arm is gradually retracted as the spacecraft approaches the Sun. This arrangement provides viewing to near 5° (i.e., includes attitude control margins and finite size of charged particle entrance apertures) inside of the edge of the heat shield umbra. The second FEA is mounted on the antiram side of the spacecraft body, pointing 180° away from the first. While the mission-unique aspects of ICARUS I will require new designs for the FIA and FEA instruments, the basic designs and subsystems can be drawn from a wide variety of previous heritage missions such as Cluster, Helios, Wind, STEREO, and Solar Orbiter.

Fast Ion Analyzer (FIA). The FIA should be capable of measuring two- and three-dimensional distribution functions for protons and alpha particles over the

energy/charge range of 50 eV/q to 20 keV/q. This energy range covers the lowest and highest expected speeds for 100 km/s protons and 1400 km/s alpha particles, respectively. The FIA's 3D temporal resolution of 3 seconds and 0.1 second for 2D distribution functions allows identification of boundaries in the solar wind down to ∼1000 km near perihelion and wave modes (e.g., the gyrofrequency is ∼300 Hz over the poles). The energy resolution ($\delta E/E$) should be approximately 5%, which does a good job of resolving the supersonic solar wind beam out to beyond 1 AU. The sensitivity and dynamic range need to be adequate to measure 2D (energy and one angle) ion distributions in 0.1s at 20 R_S without saturating the detectors all the way into perihelion. The FIA's field of view (FOV) needs to observe as much of the ram side of the viewing space as possible. To resolve the ion distributions everywhere from 0.3 AU into perihelion, FIA's angular resolution needs to be $\sim 5^\circ$ around the solar wind beam and $\sim 30^\circ$ over the remainder of its FOV.

Fast Electron Analyzer (FEA). The FEAs should be capable of measuring two-and three-dimensional electron distribution functions over the energy range from ∼1 eV to 5 keV. This energy range covers from the lowest energy photoelectrons, through the thermal core population and well up into the suprathermal halo population. The FEA's 3D temporal resolution of 3s (0.1s for 2D distribution functions of energy and one angle) is matched to the FIA to help resolve plasma conditions and structures on the same scales. The energy resolution ($\delta E/E$) should be approximately 10%, which does a good job of resolving the hot electron distributions. Like the FIA, the FEA requires a sensitivity and dynamic range adequate to measure the 2D distributions in 0.1s at 20 R_S without saturating the detectors all the way into perihelion. Together the FEAs need to observe as much of 4 steradians as possible; all-sky imagers and deflecting top-hat analyzers are both appropriate approaches for achieving the needed FOVs. To resolve possibly very narrow halo electron beams (the strahl), the FEAs need angular resolutions that approach 3° in at least one dimension at higher energies around the magnetic field direction (this information is supplied real-time from the magnetometer via the payload DPU), while ∼30° angular resolution is adequate to measure the remainder of the halo population and the core and photoelectron populations at lower energies.

2.3.2 Ion Composition Analyzer (ICA)

The ICA is supposed to be mounted, together with the FIA and one FEA, on the movable ram-facing arm referred to in Section 2.3.1. The ICA should be capable of measuring two- and three-dimensional distribution functions of He and heavy ions in the solar wind, over an energy range from ∼100 eV/q to ∼60 keV/q and a mass range from 2 amu to $\geq$ 60 amu. The required energy range covers all major solar wind species that will be observed during the solar encounter. ICA's 3D temporal resolution of 10s (at 20 R_S) permits temporal and spatial effects to be distinguished and allows comprehensive assessment of the non-thermal properties of the distribution functions that are generally expected from various solar wind acceleration and heating mechanisms. Furthermore, with the required mass range the ICA will measure species with low ionic charge states (i.e., He+) and high masses (i.e., SiO_2), such as those produced from neutral sources in the inner heliosphere or created by the

solar wind's interaction with dust near the Sun (e.g., inner source pickup ions). The energy resolution ($\delta E/E$) should be $4-5\%$, sufficient to resolve the supersonic solar wind beam out to beyond 1 AU. The sensitivity should be sufficient to measure He/O ratios every 10s at 20 R_S which can be achieved scaling from 1 AU observations of solar wind composition and charge states. The dynamic range should be $\sim 10^4 - 10^5$. The ICA FOV needs to observe as much of the ram side of the viewing space as possible due to the large amount of variability expected due to turbulence or waves in the outer corona. This can be achieved, for example, with a top-hat and swept FOV, or with an instrument with large instantaneous FOV as done on MESSENGER, provided that the edge of the FOV extends to close to the heat shield. To resolve the ion distributions everywhere from 1 AU to perihelion, ICA's angular resolution needs to be $\sim 10^\circ$ around the solar wind beam and $\sim 20^\circ$ over the remainder of its FOV.

2.3.3 Energetic Particle Instrument (EPI)

The ICARUS Energetic Particle Instrumentation (EPI) consists of a low-energy sensor (EPI-Lo) and a high-energy sensor (EPI-Hi). Both packages are to be mounted on the spacecraft body, where they view particles incident from both the sunward and anti-sunward hemispheres.

EPI Low-Energy Instrument (EPI-Lo). The EPI low-energy instrument is required to measure the composition and pitch-angle distributions of energetic particles. The composition includes hydrogen to iron as well as energetic electrons. As a minimum the detector should be able to make the ion measurements from $\sim$20 keV/nucleon to $\sim$1MeV/nucleon and the electron measurements from $\sim$25 keV to $\sim$1 MeV. Composition measurements should discriminate protons, ^{3}He, ^{4}He, C, O, Ne, Mg and Si, and Fe. The measurements should have sufficient angular spread and resolution to enable pitch-angle measurements of the differential particle fluxes for a (nominal) radial magnetic field. A "slice" field of view of $\sim 10^\circ$ wide and $> 120^\circ$ and at least 5 angular bins would suffice; at least 120° coverage and an angular resolution of no worse than 30° are required. The wider opening should be aligned with the spacecraft spin axis with the field of view just clearing the thermal protection system. Larger solid-angle coverage and better species resolution are, of course, preferred. The sensitivity should be at least ~ 1 (cm^2 sr s keV)$^{-1}$. Timing resolution should be no worse than 1s for e^-, 5s for protons, and 30s for heavier nuclei. The capabilities described here can be achieved with energetic particle instruments of the type currently being flown on MESSENGER and STEREO.

EPI High-Energy Instrument (EPI-Hi). The EPI high-energy instrument (EPI-Hi) is required to measure the composition and energy spectra of energetic nuclei with $1 < Z < 26$ from $\sim$1 to 100 MeV/nucleon, as well as energetic electrons from $\sim$0.3 to 3 MeV. The source of the energetic ions to be observed over the course of the ICARUS mission range from quiet-time intensities of cosmic rays, to low-energy ions accelerated in CIRs and transient interplanetary shocks, to ions accelerated in small, impulsive events associated with solar flares, to solar energetic particles accelerated in large gradual events. As a minimum, the charge resolution should be sufficient to measure differential intensities of H, He, C, N, O, Ne, Mg, Si, and Fe, although minor species are also of interest. It would also be very useful to include nuclei with 30

$<Z<$ 83 that are found to be enhanced in some SEP events associated with impulsive solar flares. It is required that ^{3}He and ^{4}He be separately identified whenever the ^{3}He/^{4}He ratio exceeds 1%. Assuming that onboard particle identification is used to sort species into a matrix of species versus energy bins, the energy resolution of these bins should be no worse than six intervals per decade. Near the Sun it can be expected that energetic ions may be highly anisotropic and beamed along the interplanetary magnetic field, which is expected to be on average radial at closest approach, but could be highly variable. It is therefore desirable for the EPI-Hi instrument to sample as much of 4 steradians as possible, including, in particular, the forward hemisphere. As a minimum EPI-Hi should be able to observe particles with pitch angles ranging from 30° to 120° with respect to the spacecraft Z-axis with an angular resolution no worse than 30°. EPI-Hi should have sufficient directional information to be able to determine the magnitude and direction of 3D anisotropies.

Although not well known, it is expected that the intensity of SEP events will scale with distance from the Sun (R) approximately as R^{-3} (cf. [77], and references therein). To observe particle populations that range from quiet-time levels near 1 AU to SEP events near the Sun requires a dynamic range of $\sim 10^7$. The peak intensity of a typical impulsive event at 1 AU is ~1 to 10 protons $cm^{-2}sr^{-1}s^{-1}$ >1 MeV. Scaling this to 2 R_S by R^{-3} suggests that intensities up to $\sim 10^7$ protons $cm^{-2}sr^{-1}s^{-1}$ >1 MeV should be measurable. Particle intensities should be measured with a timing resolution that is no worse than 1s for electrons, 5s for H, and 30s for Z = 2 nuclei. There is considerable heritage for energetic particle instruments in the 1–100 MeV/nucleon energy range. Instrument designs that could be adapted to meet these requirements (assuming modern, low-power, low mass electronics) have flown on Helios, Voyager, ISEE-3, Ulysses, Wind, ACE, and STEREO.

2.3.4 DC Magnetometer (MAG)

The ICARUS direct current Magnetometer (MAG) will provide context and definition of local magnetic structure and low frequency (<10 Hz) magnetic fluctuations. DC magnetic field measurements are successfully carried out onboard Solar Orbiter and Parker Solar Probe missions. The design of the instrument may be done similarly to fluxgate magnetometers used in these two missions [78–80].

MAG consists of one or more 3-axis sensors mounted close to the end of a deployable, non-retractable axial boom extending from the bottom deck of the spacecraft. (Owing to the size of the Thermal Protection System (TPS), MAG sensors can not be placed sufficiently far from the spacecraft body for a dual magnetometer configuration to be practical in removing spacecraft fields. A second MAG sensor could be used to provide low-power and low-mass redundancy.) The MAG sensor may not be located too close to the search coil component of the Radio and Plasma Wave Instrument (RPWI), making it necessary for both to work together to provide a suitable measurement environment.

Extrapolation of Helios data acquired at distances of 0.3 AU yields an average interplanetary magnetic field of approximately 260 nT at 20 R_S, the distance at which the primary mission begins and might be as high as 1–6 G at 4 R_S. MAG should be capable of switching sensitivity ranges. At least four ranges are needed, with the most

sensitive being B less than 0.1 nT and the high-field range being of the order of 8–10 G. With some adjustment to accommodate the upper range, this requirement could be met with magnetometers commonly flown on magnetospheric missions today.

2.3.5 Radio and Plasma Wave Instrument (RPWI)

The RPWI instrument may be designed similarly to the FIELDS instrument suite on Parker Solar Probe [78] and RPW instrument onboard Solar Orbiter [81].

The RPWI sensors consist of a 3-axis search coil for detecting magnetic field fluctuations and a 3-element electric field antenna system. The search coil sensor is mounted on the aft spacecraft boom, with the separation from the DC magnetometer and other instruments to minimize contamination of the search coil data to be determined. The electric field antenna system should be designed in such a way to accommodate, if possible, both DC electric field and high frequency Quasi-Thermal Noise (QTN) measurements (see Electric Field Measurements). The antenna system is mounted on the base of the spacecraft, with the three antenna elements separated by $\sim$120°. Each element may be about 1.75 m long. The antenna inclination to the spacecraft axis is varied with distance from the Sun, so as to maintain permanently some portion of it in sunlight, while minimizing heat input into the spacecraft. The portion of antenna in sunlight needs to be the same on each element in order to enable low frequency (less than 3 kHz) plasma waves to be sampled. To be accommodated safely on the spacecraft, the RPWI antenna will need to be made from a refractory material that will operate at temperatures up to 1400°C.

Search Coil Magnetic Field Measurements. The RPWI magnetic field experiment should operate in the frequency range $\sim$1 Hz to 80 kHz, allowing overlap with the DC magnetometer at low frequencies and to measure fluctuations beyond the ion cyclotron frequency at high frequencies.

Electric Field Measurements. The RPWI electric field experiment should measure fluctuations in the electric field from close to DC to above the plasma frequency (1 Hz to 30 MHz was chosen for the strawman instrument) so as to return information on low-frequency waves, turbulence, small scale structures and processes at and below the ion inertial scale. RPWI will be also designed to diagnose accurately the electron plasma parameters (density and temperature) using QTN spectroscopy. QTN requires sampling the electric field fluctuations from low frequency to above the plasma frequency. The strawman instrument has a sampling density of 40 samples per decade and a temporal sampling period of 0.1s to allow rapid sampling of plasma parameters local to the spacecraft. A sensitivity of 2×10^{-17} V/m^2/Hz at 10 MHz provides adequate signal to noise for QTN measurements. The strawman instrument returns 3-axis measurements sampled at 40 samples per decade, and as with the magnetic field, cross spectra between components are returned. In the low frequency regime ($<$10 kHz), cross spectra between E and B are measured to facilitate identification of wave modes. Waveform data that allow the study of small-scale phenomena are returned as burst mode data with a 60s cadence.

2.3.6 Neutron/Gamma-Ray Spectrometer (NGS)

The NGS instrument was described in [82]. According to our knowledge such instrument was not yet launched, but there were developments supported by CNES.

The NGS detector should be capable of detecting and positively identifying neutrons and gamma rays from the Sun having energies that range up to 10 MeV. The neutron component should be capable of intrinsic energy resolution sufficient to separate neutrons having energies below and above 1 MeV, and better than 50% energy resolution for neutron energies between 1 MeV and 10 MeV. This last requirement is needed to separate quasi-steady-state neutron emission from transient neutron emission. The NGS will measure the products of the acceleration of protons (via neutrons and gamma rays) and electrons (via gamma rays) as they interact with the dense low chromosphere and photosphere. If microflares or nanoflares play a significant role in coronal heating, these signatures of particle acceleration will be present. Their spectrum and time variation provide information on the acceleration process(es).

Upward-propagating protons and electrons may be directly detected by ICARUS I, although the probability of crossing the appropriate field lines at the critical time may be small. The neutron and gamma-ray detection suffers no such restriction. Furthermore, ICARUS's close passage to the Sun provides tremendous advantage for detection of low energy neutrons because of their short lifetimes, as well as for spectroscopy of faint gamma-ray bursts. These observations will, for the first time, provide solid statistical knowledge of frequency of energetic acceleration in small solar flares.

A detection of a burst of gamma rays would help refine the energy spectrum of transient neutrons through use of the measured time of flight between neutron arrival times and the time of the gamma-ray burst. The detection sensitivity of the NGS should be sufficient to measure neutrons produced by flares that release greater than 10^{24} ergs.

2.3.7 Common Data Processing Unit (CDPU)

For the majority of space missions (Cluster, Solar Orbiter, Parker Solar Probe), the common DPU's are used. The CDPU integrates the data processing and low voltage power conversion for all of the payload science instruments into a fully redundant system that eliminates replication, increases redundancy, and reduces overall payload resources. The CDPU provides a unified interface to the payload for the spacecraft. The spacecraft selects which side of the CDPU will be powered, leaving the redundant side off as a cold spare. The payload CDPU communicates with the spacecraft accepting commands and producing CCSDS packets ready for final processing by the spacecraft for telemetry to the ground.

3 Conclusion

ICARUS will be the first mission ever to reach the deepest layers of the solar atmosphere, exploring the least well known region of the heliosphere and offering a unique

scientific opportunity to address and answer two of the major unsolved questions in modern physics. ICARUS also represents a major technological challenge because of the scorching heat of the Sun. Recent developments in material science, however, and the return from the first solar encounters of Parker Solar Probe show that this objective is now reachable. ICARUS is the obvious next step towards the Sun, with an unequalled potential for federating the scientific community and attracting public interest.

Acknowledgements We acknowledge support from CNES for carrying out this study. SW was funded by UK STFC through grant ST/R000697/1. The authors are grateful to R. von Steiger for his kind assistance in reproducing Figure 2.

Data Availability No new data sets were created in the process of the study. All data shown are publicly available from the appropriate mission archives.

Declarations

Competing interests The authors declare that they have no competing interests

References

1. Kasper, J.C., Bale, S.D., Belcher, J.W., Berthomier, M., Case, A.W., Chandran, B.D.G., Curtis, D.W., Gallagher, D., Gary, S.P., Golub, L., Halekas, J.S., Ho, G.C., Horbury, T.S., Hu, Q., Huang, J., Klein, K.G., Korreck, K.E., Larson, D.E., Livi, R., Maruca, B., Lavraud, B., Louarn, P., Maksimovic, M., Martinovic, M., McGinnis, D., Pogorelov, N.V., Richardson, J.D., Skoug, R.M., Steinberg, J.T., Stevens, M.L., Szabo, A., Velli, M., Whittlesey, P.L., Wright, K.H., Zank, G.P., MacDowall, R.J., McComas, D.J., McNutt, R.L., Pulupa, M., Raouafi, N.E., Schwadron, N.A.: Alfvénic velocity spikes and rotational flows in the near-Sun solar wind. Nature **576**(7786), 228 (2019). https://doi.org/10.1038/s41586-019-1813-z
2. Bale, S.D., Badman, S.T., Bonnell, J.W., Bowen, T.A., Burgess, D., Case, A.W., Cattell, C.A., Chandran, B.D.G., Chaston, C.C., Chen, C.H.K., Drake, J.F., de Wit, T.D., Eastwood, J.P., Ergun, R.E., Farrell, W.M., Fong, C., Goetz, K., Goldstein, M., Goodrich, K.A., Harvey, P.R., Horbury, T.S., Howes, G.G., Kasper, J.C., Kellogg, P.J., Klimchuk, J.A., Korreck, K.E., Krasnoselskikh, V.V., Krucker, S., Laker, R., Larson, D.E., MacDowall, R.J., Maksimovic, M., Malaspina, D.M., Martinez-Oliveros, J., McComas, D.J., Meyer-Vernet, N., Moncuquet, M., Mozer, F.S., Phan, T.D., Pulupa, M., Raouafi, N.E., Salem, C., Stansby, D., Stevens, M., Szabo, A., Velli, M., Woolley, T., Wygant, J.R.: Highly structured slow solar wind emerging from an equatorial coronal hole. Nature **576**(7786), 237 (2019). https://doi.org/10.1038/s41586-019-1818-7
3. Kasper, J.C., Klein, K.G., Lichko, E., Huang, J., Chen, C.H.K., Badman, S.T., Bonnell, J., Whittlesey, P.L., Livi, R., Larson, D., Pulupa, M., Rahmati, A., Stansby, D., Korreck, K.E., Stevens, M., Case, A.W., Bale, S.D., Maksimovic, M., Moncuquet, M., Goetz, K., Halekas, J.S., Malaspina, D., Raouafi, N.E., Szabo, A., MacDowall, R., Velli, M., Dudok de Wit, T., Zank, G.P.: Parker solar

probe enters the magnetically dominated solar corona. Phys. Rev. Lett. **127**(25), 255101 (2021). https://doi.org/10.1103/PhysRevLett.127.255101
4. Fox, N.J., Velli, M.C., Bale, S.D., Decker, R., Driesman, A., Howard, R.A., Kasper, J.C., Kinnison, J., Kusterer, M., Lario, D., Lockwood, M.K., McComas, D.J., Raouafi, N.E., Szabo, A.: The Solar Probe plus mission: Humanity's first visit to our star. Space Sci. Rev. **204**(1–4), 7 (2015). https://doi.org/10.1007/s11214-015-0211-6
5. Maksimovic, M., Velli, M.: PHOIBOS: Probing heliospheric origins with an inner boundary observing spacecraft. Exp. Astron. **23**(3), 1057 (2009)
6. Müller, D., Marsden, R.G., St. Cyr, O.C., Gilbert, H.R.: Solar orbiter. Exploring the sun-heliosphere connection. Sol. Phys. **285**, 25 (2013). https://doi.org/10.1007/s11207-012-0085-7
7. Lemaire, J.F.: Determination of coronal temperatures from electron density profiles. arXiv:1112.3850 (2011)
8. Kohl, J.L., Cranmer, S., Esser, R., Gardner, L.D., Fineschi, S., Lin, J., Panasyuk, A., Raymond, J.C., Strachan, L.: Ultraviolet spectroscopy of solar energetic particle source regions. In: Fineschi, S., Viereck, R.A. (eds.) Solar Physics and Space Weather Instrumentation, vol. 5901, pp. 262–272 (2005). https://doi.org/10.1117/12.620821
9. Scudder, J.D.: Why all stars should possess circumstellar temperature inversions. Astrophys. J. **398**, 319 (1992). https://doi.org/10.1086/171859
10. Landi, S., Matteini, L., Pantellini, F.: Electron heat flux in the solar wind: are we observing the collisional limit in the 1 AU Data? Astrophys. J. Lett. **790**, L12 (2014). https://doi.org/10.1088/2041-8205/790/1/L12
11. McComas, D.J., Elliott, H.A., Schwadron, N.A., Gosling, J.T., Skoug, R.M., Goldstein, B.E.: The three-dimensional solar wind around solar maximum. Geophys. Res. Lett. **30**, 1517 (2003). https://doi.org/10.1029/2003GL017136
12. Parker, E.N.: Interaction of the solar wind with the geomagnetic field. Phys. Fluids **1**, 171 (1958)
13. Geiss, J., Gloeckler, G., Von Steiger, R.: Origin of the solar wind from composition data. Space Sci. Rev. **72**(1), 49 (1995). https://doi.org/10.1007/BF00768753
14. Shibata, K., Nakamura, T., Matsumoto, T., Otsuji, K., Okamoto, T.J., Nishizuka, N., Kawate, T., Watanabe, H., Nagata, S., UeNo, S., Kitai, R., Nozawa, S., Tsuneta, S., Suematsu, Y., Ichimoto, K., Shimizu, T., Katsukawa, Y., Tarbell, T.D., Berger, T.E., Lites, B.W., Shine, R.A., Title, A.M.: Chromospheric anemone jets as evidence of ubiquitous reconnection. Science **318**, 1591 (2007). https://doi.org/10.1126/science.1146708
15. Katsukawa, Y., Berger, T.E., Ichimoto, K., Lites, B.W., Nagata, S., Shimizu, T., Shine, R.A., Suematsu, Y., Tarbell, T.D., Title, A.M., Tsuneta, S.: Small-scale jetlike features in penumbral chromospheres. Science **318**, 1594 (2007). https://doi.org/10.1126/science.1146046
16. Li, X., Habbal, S.R., Kohl, J.L., Noci, G.: The effect of temperature anisotropy on observations of doppler dimming and pumping in the inner Corona. Astrophys. J. Lett. **501**, L133 (1998). https://doi.org/10.1086/311428
17. Kohl, J.L., Noci, G., Antonucci, E., Tondello, G., Huber, M.C.E., Cranmer, S.R., Strachan, L., Panasyuk, A.V., Gardner, L.D., Romoli, M., Fineschi, S., Dobrzycka, D., Raymond, J.C., Nicolosi, P., Siegmund, O.H.W., Spadaro, D., Benna, C., Ciaravella, A., Giordano, S., Habbal, S.R., Karovska, M., Li, X., Martin, R., Michels, J.G., Modigliani, A., Naletto, G., O'Neal, R.H., Pernechele, C., Poletto, G., Smith, P.L., Suleiman, R.M.: UVCS/SOHO empirical determinations of anisotropic velocity distributions in the solar Corona. Astrophys. J. Lett. **501**, L127 (1998). https://doi.org/10.1086/311434
18. Grall, R.R., Coles, W.A., Klinglesmith, M.T.: Observations of the solar wind speed near the sun. In: Winterhalter, D., Gosling, J.T., Habbal, S.R., Kurth, W.S., Neugebauer, M. (eds.) American Institute of Physics Conference Series, vol. 382, p. 108 (1996). https://doi.org/10.1063/1.51353
19. Raymond, J.C., Fineschi, S., Smith, P.L., Gardner, L., O'Neal, R., Ciaravella, A., Kohl, J.L., Marsden, B., Williams, G.V., Benna, C., Giordano, S., Noci, G., Jewitt, D.: Solar wind at 6.8 solar Radii from UVCS observation of comet C/1996Y1. Astrophys. J. **508**, 410 (1998). https://doi.org/10.1086/306391
20. Antonucci, E., Dodero, M.A., Giordano, S., Krishnakumar, V., Noci, G.: Spectroscopic measurement of the plasma electron density and outflow velocity in a polar coronal hole. Astron. Astrophys. **416**(2), 749 (2004). https://doi.org/10.1051/0004-6361:20031650
21. Gabriel, A.H., Abbo, L., Bely-Dubau, F., Llebaria, A., Antonucci, E.: Solar wind outflow in polar plumes from 1.05 to 2.4 R_S. Astrophys. J. **635**(2), L185 (2005). https://doi.org/10.1086/499521

22. Maksimovic, M., Velli, M.: PHOIBOS: probing heliospheric origins with an inner boundary observing spacecraft. Exp. Astron. **23**(3), 1057 (2009). https://doi.org/10.1007/s10686-008-9113-x
23. De Pontieu, B., McIntosh, S.W., Carlsson, M., Hansteen, V.H., Tarbell, T.D., Schrijver, C.J., Title, A.M., Shine, R.A., Tsuneta, S., Katsukawa, Y., Ichimoto, K., Suematsu, Y., Shimizu, T., Nagata, S.: Chromospheric Alfvénic waves strong enough to power the solar wind. Science **318**, 1574 (2007). https://doi.org/10.1126/science.1151747
24. Grappin, R., Mangeney, A., Marsch, E.: On the origin of solar wind MHD turbulence - HELIOS data revisited. J. Geophys. Res. **95**, 8197 (1990). https://doi.org/10.1029/JA095iA06p08197
25. David, C., Gabriel, A.H., Bely-Dubau, F., Fludra, A., Lemaire, P., Wilhelm, K.: Measurement of the electron temperature gradient in a solar coronal hole. Astron. Astrophys. **336**, L90 (1998)
26. Rosenbauer, H., Schwenn, R., Marsch, E., Meyer, B., Miggenrieder, H., Montgomery, M.D., Muehlhaeuser, K.H., Pilipp, W., Voges, W., Zink, S.M.: A survey on initial results of the HELIOS plasma experiment. J. Geophys. Z. Geophys. **42**, 561 (1977)
27. Scudder, J.D.: Ion and electron suprathermal tail strengths in the transition region: Support for the velocity filtration model of the corona. Astrophys. J. **427**, 446 (1994). https://doi.org/10.1086/174155
28. Maksimovic, M., Pierrard, V., Lemaire, J.F.: A kinetic model of the solar wind with Kappa distribution functions in the corona. Astron. Astrophys. **324**, 725 (1997)
29. Zouganelis, I., Maksimovic, M., Meyer-Vernet, N., Lamy, H., Issautier, K.: A transonic collisionless model of the solar wind. Astrophys. J. **606**, 542 (2004). https://doi.org/10.1086/382866
30. Matthaeus, W.H., Zank, G.P., Leamon, R.J., Smith, C.W., Mullan, D.J., Oughton, S.: Fluctuations, dissipation and heating in the corona. Space Sci. Rev. **87**, 269 (1999). https://doi.org/10.1023/A:1005125223740
31. Velli, M.: On the propagation of ideal, linear Alfven waves in radially stratified stellar atmospheres and winds. Astron. Astrophys. **270**, 304 (1993)
32. Verdini, A., Velli, M.: Alfvén waves and turbulence in the solar atmosphere and solar wind. Astrophys. J. **662**, 669 (2007). https://doi.org/10.1086/510710
33. Wilhelm, K., Curdt, W., Marsch, E., Schühle, U., Lemaire, P., Gabriel, A., Vial, J.C., Grewing, M., Huber, M.C.E., Jordan, S.D., Poland, R.J., nad Thomas, A.I., Kühne, M., Timothy, J.G., Hassler, D.M., Siegmund, O.H.W.: SUMER - solar ultraviolet measurements of emitted radiation. Solar Phys. **162**(1), 189 (1995). https://doi.org/10.1007/BF00733430
34. Banerjee, D., Teriaca, L., Doyle, J.G., Wilhelm, K.: Broadening of SI VIII lines observed in the solar polar coronal holes. Astron. Astrophys. **339**, 208 (1998)
35. Esser, R., Fineschi, S., Dobrzycka, D., Habbal, S.R., Edgar, R.J., Raymond, J.C., Kohl, J.L., Guhathakurta, M.: Plasma properties in coronal holes derived from measurements of minor ion spectral lines and polarized white light intensity. Astrophys. J. **510**(1), L63 (1999). https://doi.org/10.1086/311786
36. Armstrong, J.W., Woo, R.: Solar wind motion within 30 R_{sun}: Spacecraft radio scintillation observations. Astron. Astrophys. **103**, 415 (1981)
37. Canals, A., Breen, A.R., Ofman, L., Moran, P.J., Fallows, R.A.: Estimating random transverse velocities in the fast solar wind from EISCAT interplanetary scintillation measurements. Ann. Geophys. **20**(9), 1265 (2002). https://doi.org/10.5194/angeo-20-1265-2002
38. Bavassano, B., Pietropaolo, E., Bruno, R.: On the evolution of outward and inward Alfvénic fluctuations in the polar wind. J. Geophys. Res. (Space Phys.) **105**(A7), 15959 (2000). https://doi.org/10.1029/1999JA000276
39. Verdini, A., Velli, M.: Alfvén waves and turbulence in the solar atmosphere and solar wind. Astrophys. J. **662**(1), 669 (2007). https://doi.org/10.1086/510710
40. Matthaeus, W.H., Mullan, D.J., Dmitruk, P., Milano, L., Oughton, S.: MHD turbulence and heating of the open field-line solar corona. Nonlinear Process. Geophys. **10**, 93 (2003)
41. Sittler Jr, E.C., Guhathakurta, M.: Erratum: Semiempirical two-dimensional magnetohydrodynamic model of the solar corona and interplanetary medium. Astrophys. J. **564**, 1062 (2002). https://doi.org/10.1086/324303
42. Teriaca, L., Poletto, G., Romoli, M., Biesecker, D.: Solar wind acceleration in low density regions. In: Velli, M., Bruno, R., Malara, F., Bucci, B. (eds.) Solar Wind Ten, pp. 327–330. American Institute of Physics Conference Series (2003). https://doi.org/10.1063/1.1618605
43. Sheeley, N.R., Wang, Y.M., Hawley, S.H., Brueckner, G.E., Dere, K.P., Howard, R.A., Koomen, M.J., Korendyke, C.M., Michels, D.J., Paswaters, S.E., Socker, D.G., St. Cyr, O.C., Wang, D., Lamy, P.L.,

Llebaria, A., Schwenn, R., Simnett, G.M., Plunkett, S., Biesecker, D.A.: Measurements of flow speeds in the corona between 2 and 30 R_s. Astrophys. J. **484**, 472 (1997)
44. Habbal, S.R., Woo, R., Fineschi, S., O'Neal, R., Kohl, J., Noci, G., Korendyke, C.: Origins of the slow and the ubiquitous fast solar wind. Astrophys. J. **489**(1), L103 (1997). https://doi.org/10.1086/310970
45. Wang, Y.M., Sheeley Jr., N.R., Phillips, J.L., Goldstein, B.E.: Solar wind stream interactions and the wind speed-expansion factor relationship. Astrophys. J. Lett. **488**, L51 (1997). https://doi.org/10.1086/310918
46. Noci, G., Kohl, J.L., Antonucci, E., Tondello, G., Huber, M.C.E., Fineschi, S., Gardner, L.D., Naletto, G., Nicolosi, P., Raymond, J.C., Romoli, M., Spadaro, D., Siegmund, O.H.W., Benna, C., Ciaravella, A., Giordano, S., Michels, J., Modigliani, A., Panasyuk, A., Pernechele, C., Poletto, G., Smith, P.L., Strachan, L.: First results from UVCS/SOHO. Adv. Space Res. **20**, 2219 (1997). https://doi.org/10.1016/S0273-1177(97)00895-8
47. Smith, E.J.: The heliospheric current sheet. J. Geophys. Res. **106**, 15819 (2001). https://doi.org/10.1029/2000JA000120
48. Neugebauer, M.: The quasi-stationary and transient states of the solar wind. Science **252**, 404 (1991). https://doi.org/10.1126/science.252.5004.404
49. Feldman, W.C., Habbal, S.R., Hoogeveen, G., Wang, Y.M.: Experimental constraints on pulsed and steady state models of the solar wind near the Sun. J. Geophys. Res. **102**, 26905 (1997). https://doi.org/10.1029/97JA02436
50. Coles, W.A., Esser, R., Lovhaug, U.P., Markkanen, J.: Comparison of solar wind velocity measurements with a theoretical acceleration model. J. Geophys. Res. **96**, 13 (1991). https://doi.org/10.1029/91JA01254
51. Feldman, W.C., Barraclough, B.L., Phillips, J.L., Wang, Y.M.: Constraints on high-speed solar wind structure near its coronal base: a ULYSSES perspective. Astron. Astrophys. **316**, 355 (1996)
52. Fisk, L.A., Kasper, J.C.: Global circulation of the open magnetic flux of the Sun. Astrophys. J. Lett. **894**(1), L4 (2020). https://doi.org/10.3847/2041-8213/ab8acd
53. Badman, S.T., Bale, S.D., Martínez Oliveros, J.C., Panasenco, O., Velli, M., Stansby, D., Buitrago-Casas, J.C., Réville, V., Bonnell, J.W., Case, A.W., Dudok de Wit, T., Goetz, K., Harvey, P.R., Kasper, J.C., Korreck, K.E., Larson, D.E., Livi, R., MacDowall, R.J., Malaspina, D.M., Pulupa, M., Stevens, M.L., Whittlesey, P.L.: Magnetic connectivity of the ecliptic plane within 0.5 AU: potential field source surface modeling of the first parker solar probe encounter. Astrophys. J. Suppl. Ser **246**(2), 23 (2020). https://doi.org/10.3847/1538-4365/ab4da7
54. Cohen, C.M.S., Mewaldt, R.A., Leske, R.A., Cummings, A.C., Stone, E.C., Wiedenbeck, M.E., Christian, E.R., von Rosenvinge, T.T.: New observations of heavy-ion-rich solar particle events from ACE. Geophys. Res. Lett. **26**, 2697 (1999). https://doi.org/10.1029/1999GL900560
55. Cane, H.V., von Rosenvinge, T.T., Cohen, C.M.S., Mewaldt, R.A.: Two components in major solar particle events. Geophys. Res. Lett. **30**, 8017 (2003). https://doi.org/10.1086/382651
56. Tylka, A.J., Cohen, C.M.S., Dietrich, W.F., Lee, M.A., Maclennan, C.G., Mewaldt, R.A., Ng, C.K., Reames, D.V.: Shock geometry, seed populations, and the origin of variable elemental composition at high energies in large gradual solar particle events. Astrophys. J. **625**, 474 (2005). https://doi.org/10.1086/429384
57. Gloeckler, G., Fisk, L.A., Zurbuchen, T.H., Schwadron, N.A.: Sources, injection and acceleration of heliospheric ion populations. In: Mewaldt, R.A., Jokipii, J.R., Lee, M.A., Möbius, E., Zurbuchen, T.H. (eds.) Acceleration and Transport of Energetic Particles Observed in the Heliosphere, American Institute of Physics Conference Series, vol. 528, pp. 221–228. American Institute of Physics Conference Series (2000). https://doi.org/10.1063/1.1324316
58. Ruffolo, D., Tooprakai, P., Rujiwarodom, M., Khumlumlert, T., Wechakama, M., Bieber, J.W., Evenson, P., Pyle, R.: Relativistic solar protons on 1989 October 22: injection and transport along both legs of a closed interplanetary magnetic loop. Astrophys. J. **639**, 1186 (2006). https://doi.org/10.1086/499419
59. Krucker, S., Christe, S., Lin, R.P., Hurford, G.J., Schwartz, R.A.: Hard X-ray Microflares down to 3 keV. Solar Phys. **210**(1), 445 (2002). https://doi.org/10.1023/A:1022404512780
60. Kahler, S.W., Reames, D.V., Sheeley Jr, N.R.: Coronal mass ejections associated with impulsive solar energetic particle events. Astrophys. J. **562**, 558 (2001). https://doi.org/10.1086/323847
61. Mason, G.M., Mazur, J.E., Dwyer, J.R.: 3He enhancements in large solar energetic particle events. Astrophys. J. **525**, L133 (1999). https://doi.org/10.1086/312349

62. Gopalswamy, N., Yashiro, S., Michałlek, G., Kaiser, M.L., Howard, R.A., Reames, D.V., Leske, R., von Rosenvinge, T.: Interacting coronal mass ejections and solar energetic particles. Astrophys. J. **572**, L103 (2002). https://doi.org/10.1086/341601
63. Li, G., Zank, G.P.: Mixed particle acceleration at CME-driven shocks and flares. Geophys. Res. Lett. **32**, L02101 (2005). https://doi.org/10.1029/2004GL021250
64. Cliver, E.W., Kahler, S.W., Reames, D.V.: Coronal shocks and solar energetic proton events. Astrophys. J. **605**, 902 (2004). https://doi.org/10.1086/382651
65. Kahler, S.W., Reames, D.V.: Solar energetic particle production by coronal mass ejection-driven shocks in solar fast-wind regions. Astrophys. J. **584**, 1063 (2003). https://doi.org/10.1086/345780
66. Mewaldt, R.A., Cohen, C.M.S., Haggerty, D.K., Gold, R.E., Krimigis, S.M., Leske, R.A., Ogliore, R.C., Roelof, E.C., Stone, E.C., von Rosenvinge, T.T., Wiedenbeck, M.E.: Heavy Ion and electron release times. In: Solar Particle Events, International Cosmic Ray Conference, vol. 6, p. 3313 (2003)
67. Gopalswamy, N., Lara, A., Kaiser, M.L., Bougeret, J.L.: Near-Sun and near-Earth manifestations of solar eruptions. J. Geophys. Res. **106**, 25261 (2001). https://doi.org/10.1029/2000JA004025
68. Zank, G.P., Rice, W.K.M., Wu, C.C.: Particle acceleration and coronal mass ejection driven shocks: A theoretical model. J. Geophys. Res. **105**, 25079 (2000). https://doi.org/10.1029/1999JA000455
69. Sokolov, I.V., Roussev, I.I., Gombosi, T.I., Lee, M.A., Kóta, J., Forbes, T.G., Manchester, W.B., Sakai, J.I.: A new field line advection model for solar particle acceleration. Astrophys. J. **616**, L171 (2004). https://doi.org/10.1086/426812
70. Feynman, J., Gabriel, S.B.: On space weather consequences and predictions. J. Geophys. Res. **105**, 10543 (2000). https://doi.org/10.1029/1999JA000141
71. McKibben, R.B., Lopate, C., Zhang, M.: Simultaneous observations of solar energetic particle events by IMP 8 and the Ulysses cospin high energy telescope at high solar latitudes. Space Sci. Rev. **97**, 257 (2001). https://doi.org/10.1023/A:1011816715390
72. Dalla, S., Balogh, A., Heber, B., Lopate, C., McKibben, R.B.: Observation of decay phases of solar energetic particle events at 1 and 5 AU from the Sun. J. Geophys. Res. (Space Physics) **107**, 1370 (2002). https://doi.org/10.1029/2001JA009155
73. Krucker, S., Lin, R.P.: Two classes of solar proton events derived from onset time analysis. Astrophys. J. **542**, L61 (2000). https://doi.org/10.1086/312922
74. Haggerty, D.K., Roelof, E.C.: Impulsive near-relativistic solar electron events: delayed injection with respect to solar electromagnetic emission. Astrophys. J. **579**(2), 841 (2002). https://doi.org/10.1086/342870
75. Cranmer, S.R., van Ballegooijen, A.A.: On the generation, propagation, and reflection of Alfvé n waves from the solar photosphere to the distant heliosphere. Astrophys. J. Suppl. Ser. **156**, 265 (2005). https://doi.org/10.1086/426507
76. Owen, C.J., Bruno, R., Livi, S., Louarn, P., Al Janabi, K., Allegrini, F., Amoros, C., Baruah, R., Barthe, A., Berthomier, M., Bordon, S., Brockley-Blatt, C., Brysbaert, C., Capuano, G., Collier, M., DeMarco, R., Fedorov, A., Ford, J., Fortunato, V., Fratter, I., Galvin, A.B., Hancock, B., Heirtzler, D., Kataria, D., Kistler, L., Lepri, S.T., Lewis, G., Loeffler, C., Marty, W., Mathon, R., Mayall, A., Mele, G., Ogasawara, K., Orlandi, M., Pacros, A., Penou, E., Persyn, S., Petiot, M., Phillips, M., Přech, L., Raines, J.M., Reden, M., Rouillard, A.P., Rousseau, A., Rubiella, J., Seran, H., Spencer, A., Thomas, J.W., Trevino, J., Verscharen, D., Wurz, P., Alapide, A., Amoruso, L., André, N., Anekallu, C., Arciuli, V., Arnett, K.L., Ascolese, R., Bancroft, C., Bland, P., Brysch, M., Calvanese, R., Castronuovo, M., Čermák, I., Chornay, D., Clemens, S., Coker, J., Collinson, G., D'Amicis, R., Dandouras, I., Darnley, R., Davies, D., Davison, G., De Los Santos, A., Devoto, P., Dirks, G., Edlund, E., Fazakerley, A., Ferris, M., Frost, C., Fruit, G., Garat, C., Génot, V., Gibson, W., Gilbert, J.A., de Giosa, V., Gradone, S., Hailey, M., Horbury, T.S., Hunt, T., Jacquey, C., Johnson, M., Lavraud, B., Lawrenson, A., Leblanc, F., Lockhart, W., Maksimovic, M., Malpus, A., Marcucci, F., Mazelle, C., Monti, F., Myers, S., Nguyen, T., Rodriguez-Pacheco, J., Phillips, I., Popecki, M., Rees, K., Rogacki, S.A., Ruane, K., Rust, D., Salatti, M., Sauvaud, J.A., Stakhiv, M.O., Stange, J., Stubbs, T., Taylor, T., Techer, J.D., Terrier, G., Thibodeaux, R., Urdiales, C., Varsani, A., Walsh, A.P., Watson, G., Wheeler, P., Willis, G., Wimmer-Schweingruber, R.F., Winter, B., Yardley, J., Zouganelis, I.: The solar orbiter solar wind analyser (SWA) suite. Astron. Astrophys. **642**, A16 (2020). https://doi.org/10.1051/0004-6361/201937259
77. Reames, D.V., Ng, C.K.: Streaming-limited intensities of solar energetic particles. Astrophys. J. **504**(2), 1002 (1998). https://doi.org/10.1086/306124
78. Bale, S.D., Goetz, K., Harvey, P.R., Turin, P., Bonnell, J.W., Dudok de Wit, T., Ergun, R.E., MacDowall, R.J., Pulupa, M., Andre, M., Bolton, M., Bougeret, J.L., Bowen, T.A., Burgess, D., Cattell,

C.A., Chandran, B.D.G., Chaston, C.C., Chen, C.H.K., Choi, M.K., Connerney, J.E., Cranmer, S., Diaz-Aguado, M., Donakowski, W., Drake, J.F., Farrell, W.M., Fergeau, P., Fermin, J., Fischer, J., Fox, N., Glaser, D., Goldstein, M., Gordon, D., Hanson, E., Harris, S.E., Hayes, L.M., Hinze, J.J., Hollweg, J.V., Horbury, T.S., Howard, R.A., Hoxie, V., Jannet, G., Karlsson, M., Kasper, J.C., Kellogg, P.J., Kien, M., Klimchuk, J.A., Krasnoselskikh, V.V., Krucker, S., Lynch, J.J., Maksimovic, M., Malaspina, D.M., Marker, S., Martin, P., Martinez-Oliveros, J., McCauley, J., McComas, D.J., McDonald, T., Meyer-Vernet, N., Moncuquet, M., Monson, S.J., Mozer, F.S., Murphy, S.D., Odom, J., Oliverson, R., Olson, J., Parker, E.N., Pankow, D., Phan, T., Quataert, E., Quinn, T., Ruplin, S.W., Salem, C., Seitz, D., Sheppard, D.A., Siy, A., Stevens, K., Summers, D., Szabo, A., Timofeeva, M., Vaivads, A., Velli, M., Yehle, A., Werthimer, D., Wygant, J.R.: The FIELDS instrument suite for solar probe plus. Measuring the coronal plasma and magnetic field, plasma waves and turbulence, and radio signatures of solar transients. Space Sci. Rev. **204**(1-4), 49 (2016). https://doi.org/10.1007/s11214-016-0244-5

79. MacDowall, R.J., Sheppard, D., Odom, J., Murphy, S., Oliversen, R.J., Choi, M.K., Lawton, P., Bickel, E.A., Bale, S.D., Goetz, K., Harvey, P.: First results from the fluxgate magnetometers (MAGs) on Parker Solar Probe. In: AGU Fall Meeting Abstracts, vol. 2018, pp. SH51B–2815 (2018)
80. Horbury, T.S., O'Brien, H., Carrasco Blazquez, I., Bendyk, M., Brown, P., Hudson, R., Evans, V., Oddy, T.M., Carr, C.M., Beek, T.J., Cupido, E., Bhattacharya, S., Dominguez, J.A., Matthews, L., Myklebust, V.R., Whiteside, B., Bale, S.D., Baumjohann, W., Burgess, D., Carbone, V., Cargill, P., Eastwood, J., Erdös, G., Fletcher, L., Forsyth, R., Giacalone, J., Glassmeier, K.H., Goldstein, M.L., Hoeksema, T., Lockwood, M., Magnes, W., Maksimovic, M., Marsch, E., Matthaeus, W.H., Murphy, N., Nakariakov, V.M., Owen, C.J., Owens, M., Rodriguez-Pacheco, J., Richter, I., Riley, P., Russell, C.T., Schwartz, S., Vainio, R., Velli, M., Vennerstrom, S., Walsh, R., Wimmer-Schweingruber, R.F., Zank, G., Müller, D., Zouganelis, I., Walsh, A.P.: The Solar Orbiter magnetometer. A&A **642**, A9 (2020). https://doi.org/10.1051/0004-6361/201937257
81. Maksimovic, M., Bale, S.D., Chust, T., Khotyaintsev, Y., Krasnoselskikh, V., Kretzschmar, M., Plettemeier, D., Rucker, H.O., Souček, J., Steller, M., Štverák, Š., Trávníček, P., Vaivads, A., Chaintreuil, S., Dekkali, M., Alexandrova, O., Astier, P.A., Barbary, G., Bérard, D., Bonnin, X., Boughedada, K., Cecconi, B., Chapron, F., Chariet, M., Collin, C., de Conchy, Y., Dias, D., Guéguen, L., Lamy, L., Leray, V., Lion, S., Malac-Allain, L.R., Matteini, L., Nguyen, Q.N., Pantellini, F., Parisot, J., Plasson, P., Thijs, S., Vecchio, A., Fratter, I., Bellouard, E., Lorfèvre, E., Danto, P., Julien, S., Guilhem, E., Fiachetti, C., Sanisidro, J., Laffaye, C., Gonzalez, F., Pontet, B., Quéruel, N., Jannet, G., Fergeau, P., Brochot, J.Y., Cassam-Chenai, G., Dudok de Wit, T., Timofeeva, M., Vincent, T., Agrapart, C., Delory, G.T., Turin, P., Jeandet, A., Leroy, P., Pellion, J.C., Bouzid, V., Katra, B., Piberne, R., Recart, W., Santolík, O., Kolmašová, I., Krupař, V., Krupařová, O., Píša, D., Uhlíř, L., Lán, R., Baše, J., Ahlèn, L., André, M., Bylander, L., Cripps, V., Cully, C., Eriksson, A., Jansson, S.E., Johansson, E.P.G., Karlsson, T., Puccio, W., Břínek, J., Öttacher, H., Panchenko, M., Berthomier, M., Goetz, K., Hellinger, P., Horbury, T.S., Issautier, K., Kontar, E., Krucker, S., Le Contel, O., Louarn, P., Martinović, M., Owen, C.J., Retinò, A., Rodríguez-Pacheco, J., Sahraoui, F., Wimmer-Schweingruber, R.F., Zaslavsky, A., Zouganelis, I.: The solar orbiter radio and plasma waves (RPW) instrument. Astron. Astrophys. **642**, A12 (2020). https://doi.org/10.1051/0004-6361/201936214, https://hal.archives-ouvertes.fr/hal-02954313
82. Vilmer, N., Maksimovic, M., Trottet, G.: Low energy neutron measurements aboard encounter missions. In: 35th COSPAR Scientific Assembly, vol. 35, p. 2018 (2004)

Affiliations

Vladimir Krasnoselskikh[1] · Bruce T. Tsurutani[2] · Thierry Dudok de Wit[1,3] · Simon Walker[4] · Michael Balikhin[4] · Marianne Balat-Pichelin[5] · Marco Velli[6] · Stuart D. Bale[7] · Milan Maksimovic[8] · Oleksiy Agapitov[7] · Wolfgang Baumjohann[9] · Matthieu Berthomier[10] · Roberto Bruno[11] · Steven R. Cranmer[12] · Bart de Pontieu[13] · Domingos de Sousa Meneses[14] · Jonathan Eastwood[15] · Robertus Erdelyi[16] · Robert Ergun[12] · Viktor Fedun[4] · Natalia Ganushkina[17] · Antonella Greco[18] · Louise Harra[19] · Pierre Henri[1] · Timothy Horbury[15] · Hugh Hudson[20] · Justin Kasper[17] · Yuri Khotyaintsev[21] · Matthieu Kretzschmar[1] · Säm Krucker[22] · Harald Kucharek[23] · Yves Langevin[24] · Benoît Lavraud[25] · Jean-Pierre Lebreton[1] · Susan Lepri[26] · Michael Liemohn[26] · Philippe Louarn[25] · Eberhard Moebius[27] · Forrest Mozer[7] · Zdenek Nemecek[28] · Olga Panasenco[29] · Alessandro Retino[10] · Jana Safrankova[28] · Jack Scudder[30] · Sergio Servidio[31] · Luca Sorriso-Valvo[32] · Jan Souček[33] · Adam Szabo[34] · Andris Vaivads[35] · Grigory Vekstein[36] · Zoltan Vörös[37] · Teimuraz Zaqarashvili[38] · Gaetano Zimbardo[18] · Andrei Fedorov[39]

2 Jet Propulsion Laboratory, California Institute of Technology, Pasadena, CA, USA

3 ISSI, Bern, Switzerland

4 Department of Automatic Control & Systems Engineering, The University of Sheffield, Sheffield, UK

5 PROMES, CNRS, Font Romeu Odeillo, France

6 EPSS, UCLA, Los Angeles, LA, USA

7 Space Sciences Laboratory, University of California, Berkeley, CA, USA

8 LESIA, Paris Observatory, Meudon, France

9 Space Research Institute / IWF Austrian Academy of Sciences, Graz, Austria

10 LPP, CNRS/Ecole Polytechnique, Palaiseau, France

11 INAF-Istituto di Astrofisica e Planetologia Spaziali, Rome, Italy

12 Department of Astrophysical and Planetary Sciences, LASP, University of Colorado, Boulder, CO, USA

13 Lockheed Martin Solar, Astrophysics Laboratory, Palo Alto, CA, USA

14 CEMHTI, CNRS, Orléans, France

15 The Blackett Laboratory, Imperial College, London, UK

16 Solar Physics and Space Plasma Research Centre, University of Sheffield, Sheffield, UK

17 Department of Atmospheric, Oceanic and Space Sciences, University of Michigan, Ann Arbor, MI, USA

18 Dipartimento di Fisica, Università della Calabria, Rende, Italy

19 PMOD/WRC, Davos, Switzerland

20 Space Sciences Laboratory, University of California, Berkeley, CA, USA

21 Swedish Institute of Space Physics, Uppsala, Sweden

22 University of Applied Sciences and Arts Northwestern Switzerland, Windisch, Switzerland

23 University of New Hampshire, Durham, NC, USA

24 IAS, CNRS/Université Paris Sud, Orsay, France

[25] IRAP, CNRS/CNES, Toulouse, France

[26] Climate and Space Sciences and Engineering, University of Michigan, Ann Arbor, MI, USA

[27] Space Science Center and Department of Physics, University of New Hampshire, Durham, NC, USA

[28] Charles University, Prague, Czech Republic

[29] Advanced Heliophysics Inc., Los Angeles, LA, USA

[30] Department of Physics and Astronomy, University of Iowa, Iowa City, IA, USA

[31] Dipartimento di Fisica, Universitá della Calabria, Cosenza, Italy

[32] Nanotec/CNR, U.O.S. LICRYL di Cosenza, Ponte P. Bucci, Cubo 31C, Rende, CS, Italy

[33] Institute of Atmospheric Physics, Academy of Sciences of the Czech Republic, Prague, Czech Republic

[34] Heliospheric Physics Laboratory, Code 672, NASA Goddard Space Flight Center, Greenbelt, MD, USA

[35] Swedish Institute of Space Physics, Uppsala, Sweden

[36] Jodrell Bank Centre for Astrophysics, University of Manchester, Manchester, UK

[37] Space Research Institute, Austrian Academy of Sciences, Graz, Austria

[38] Institute of Physics, IGAM, University of Graz, Graz, Austria

[39] IRAP, OMP, Toulouse, France